

Kriyojenik işlem görmüş AM60 ve AZ91 alařımlarının korozyon ve aşınma karakterizasyonu

Basady GASSAMA

YÜKSEK LİSANS TEZİ

Havacılık Bilimi ve Teknolojileri Anabilim Dalı

Ağustos 2020

Corrosion and Wear Characterization of Cryogenic Treated AM60 and AZ91 Alloys

Basady GASSAMA

MASTER OF SCIENCE THESIS

Department of Aviation Science and Technologies

August 2020

Corrosion and Wear Characterization of Cryogenic Treated AM60 and AZ91 Alloys

Basady GASSAMA

A thesis submitted to Eskişehir Osmangazi University
Graduate School of Natural and Applied Sciences in partial
fulfillment of the requirements for the degree of Master of Science
in Department of Aviation Science and Technologies

Supervisor: Doç. Dr. Mustafa Özgür ÖTEYAKA

August 2020

ETHICAL STATEMENT

I hereby declare that this thesis study entitled “Kriyojenik işlem görmüş AM60 ve AZ91 alaşımlarının korozyon ve aşınma karakterizasyonu” has been prepared in accordance with the thesis writing rules of Eskişehir Osmangazi University Graduate School of Natural and Applied Sciences under academic consultancy of my supervisor Assoc. Prof. Dr. Mustafa Özgür ÖTEYAKA. I hereby declare that the work presented in this thesis is original. I also declare that, I have respected scientific ethical principle and rules in all stages of my thesis study, all information and data presented in this thesis have been obtained within the scope of scientific and academic ethical principles and rules, all materials used in this thesis which are not original to this work have been fully cited and referenced, and all knowledge, documents and results have been presented in accordance with scientific ethical principles and rules. 21/08/2020

Basady GASSAMA

ÖZET

Bu çalışmada, -196 °C'de 48 saat kriyojenik işlem görmüş ve görmemiş AZ91 ve AM60 magnezyum alaşımlarının korozyon ve aşınma özellikleri incelenmiştir. Bu malzemelerin korozyon performansı, ağırlıkça % 0.9 NaCl içeren izotonik çözeltide test edildi. Korozyon performansını değerlendirmek için açık devre potansiyel ölçümü (OCP), potansiyodinamik polarizasyonu, dönüşümlü voltametri (CV) ve elektrokimyasal empedans spektroskopisi (EIS) gibi elektrokimyasal yöntemler kullanılmıştır. Öte yandan, AZ91 ve AM60 magnezyum alaşımlarının aşınma performansı 1 N, 3 N ve 5 N yükleri altında kuru ve ağırlıkça % 0.9 NaCl izotonik çözelti ortamında tribometre (pin-on-disk metodu) kullanılarak araştırılmıştır.

Yapılan çalışma sonucunda, kriyojenik işlem görmüş AZ91 ve AM60 numunelerinin işlem görmemiş numuneye kıyasla üstün korozyon direncine sahip olduğunu göstermektedir. OCP sonuçları, kriyojenik olarak muamele edilmiş AZ91 ve AM60 alaşımlarının 1 saat sonra ısıtılmış işlem görmemiş numunelere göre daha iyi performans gösterdiği saptanmıştır. Diğer taraftan, kriyojenik olarak işle görmüş AZ91 ve AM60'ın pasivasyon bölgesinin geniş ve anodik çukurlaşma potansiyelinin (E_{pit}) işlem görmemiş numunelere göre anodik olduğu gözlemlenmiştir. Ayrıca, kriyojenik ısıtılmış işlem görmüş numuneler AZ91 ve AM60 alaşımlarının düşük korozyon reaksiyonlarına sahip olduğu EIS yöntemiyle tespit edilmiştir. Aşınma testinde, aşınma izlerinin artan yük ile beraber genişliğinin arttığını tüm numuneler için görülmüştür. Bunun yanında, düşük (1 N) ve orta yükte (3 N) ısıtılmış işlem görmüş numunelerin aşınmaya karşı daha dirençli olduğu tespit edilmiştir. Kuru ortamda kriyojenik işlem görmüş numunelerin aşınmaya karşı daha dirençli fakat ağırlıkça % 0.9 NaCl çözelti ortamında ısıtılmış işlem görmemiş numunelere göre aşınmalarının zayıf olduğu belirlenmiştir.

Anahtar Kelimeler: Kriyojenik işlem, Korozyon, AZ91, AM60, Aşınma, Magnezyum.

SUMMARY

In this study, untreated and cryogenically treated at -196°C for 48 h AZ91 and AM60 magnesium alloy were employed. The corrosion performance of the AZ91 and AM60 samples was tested in isotonic solution containing 0.9% NaCl. Electrochemical methods such as the open-circuit potential measurement (OCP), potentiodynamic polarization, cyclic voltammetry (CV), and electrochemical impedance spectroscopy (EIS) were used to evaluate the corrosion performance. On the other hand, wear behavior performance of AZ91 and AM60 magnesium alloy were investigated in a dry and in 0.9 wt. % NaCl medium. The wear performance is investigated under loads of 1 N, 3 N, and 5 N using a tribometer (pin-on-disc method) and profilometer for each sample in both medium. An optic microscope is used to examine the forms of wear endured and to measure the width of the wear track to determine the depth of penetration in comparison to the samples. The analysis of variance method is also performed to find the relationship between parameters.

The results show that the cryogenically treated AZ91 and AM60 samples hold superior corrosion resistance when compared to the former sample. The OCP results indicated that the cryogenically treated AZ91 and AM60 outperformed untreated samples after 1 h. The potentiodynamic studies presented that cryogenically treated AZ91 and AM60 had superior anodic pitting potential (Epit) and that the passivation zone is higher than AZ91 and AM60 when untreated. The EIS confirmed lower corrosion kinetics for AZ91 and AM60 treated in the former sample. Regarding to wear behavior, it was observed for all samples that the width of the wear tracks increased with increasing load. In addition, heat treated samples at low (1 N) and medium load (3 N) were found to be more resistant to abrasion. It has been determined that the samples that are cryogenic treated are more resistant to abrasion in dry environment, but they are weak in 0.9 wt. % NaCl solution medium in comparison with the samples that have not been heat treated.

Keywords: Cryogenic Treatment, Corrosion, AZ91, AM60, Wear, Magnesium.

ACKNOWLEDGEMENT



LIST OF CONTENTS

	<u>Page</u>
ÖZET.....	Vi
SUMMARY.....	Vii
ACKNOWLEDGEMENTS.....	Viii
LIST OF CONTENTS.....	ix
LIST OF FIGURES.....	X
LIST OF TABLES.....	Xii
1. INTRODUCTION AND PURPOSE.....	1
2. LITERATURE REVIEW.....	4
2.1. Magnesium and its Alloys.....	4
2.2. Properties of Magnesium	6
2.3. Effect of Alloying Element on Magnesium	8
2.4. Cryogenic Treatment.....	10
2.5. Corrosion Behaviour of Magnesium Alloys	12
2.6. Wear Behaviour of Magnesium Alloys.....	14
3. MATERIALS AND METHODS.....	16
3.1. Materials Preparation	16
3.2. Cryogenic Treatment.....	16
3.3. Electrochemical Test.....	17
3.4. Wear Test	18
4. RESULTS AND DISCUSSIONS	19
4.1. Effect of Treatment on the Microstructure.....	19
4.2. Electrochemical Results	20
4.2.1. Open circuit potential (OCP).....	20
4.2.2. Potentiodynamic and cyclic voltammetry	22
4.2.3. Electrochemical impedance spectroscopy (EIS) analysis	24
4.3. Wear Test Results.....	26
4.3.1. Optic microscope images of worn surfaces.....	26
4.3.2. Specific wear rate and coefficient of friction behaviour	32
5. CONCLUSIONS AND RECOMMENDATIONS	45
REFERENCES.....	48

LIST OF FIGURES

<u>Figure</u>	<u>Page</u>
2.1. Examples of application for magnesium alloys in Boeing 747: wing and seat components (Dziubińska 2016).....	5
2.2. Air conditioning system made of magnesium alloy WE43 for aircraft (Dziubińska et al., 2016).	5
2.3. Magnesium hexagonal close-packed crystal structure (Callister 2020).	7
2.4. General cycle of cryogenic treatment (Sonar 2018).	11
2.5. Modification of the atom structure (Sonar et al., 2018).	11
2.6. SRET maps for a) AZ91E and b) ZACS1040305 in 5% NaCl solution saturated with Mg(OH) ₂ at pH = 9 and 25°C for 3 different time periods (Klassen et al., 2005).	13
2.7. a) potentiodynamic behaviour of the AZ91E and ZAC10403 alloys in the 5% NaCl solution saturated with Mg(OH) ₂ at pH = 9 and 25°C; b) Corroded surface of AZ91E and ZAC10403 (Öteyaka et al., 2003).	13
2.8. The influence of load on the hot rolled AZ31 alloy with differen velocity (Mert 2017). ..	14
2.9. SEM images showing the delamination of hot rolled AZ31 after at load 40 N and velocity of 1 m/s (Mert 2017).....	15
3.1. Cryogenic treatment setup.	17
3.2. Electrochemical setup.....	17
3.3. Wear setup.	18
4.1. Optic images of AZ91 and AM60 at magnification of x500; a) AZ91 untreated b) AZ91 cryogenic treated c) AM60 untreated d) AM60 cryogenic treated.	20
4.2. The Ecorr/time plots of untreated and treated of AZ91 and AM60 in isotonic solution.....	21
4.3. Polarization curves of the untreated and treated AZ91 and AM60 alloys in the isotonic solution (scan rate 5 mV/s).	23
4.4. The cyclic voltammetry behavior of cryogenic-treated and non-treated AZ91 and AM60 alloys in the isotonic solution.	24
4.5. Nyquist plot of the untreated and cryogenic treated Az91 and AM60 alloys in an isotonic solution.	25
4.6. Worn surfaces of untreated and cryogenic treated AZ91 wear tracks in a dry medium. ...	27

LIST OF FIGURES (continue)

<u>Figure</u>	<u>Page</u>
4.7. Worn surfaces of untreated and cryogenic treated AZ91 wear tracks in a wet medium.	29
4.8. Worn surfaces of untreated and cryogenic treated AM60 wear tracks in a dry medium. ..	30
4.9. Worn surfaces of untreated and cryogenic treated AM60 wear tracks in a wet medium. ...	32
4.10. A cross-sectional view of untreated and cryogenic treated AZ91 wear track profiles in a dry medium.	33
4.11. A cross-sectional view of untreated and cryogenic treated AZ91 wear track profiles in a wet medium.	34
4.12. A cross-sectional view of untreated and cryogenic treated AM60 wear track profiles in a dry medium.	35
4.13. A cross-sectional view of untreated and cryogenic treated AZ91 wear track profiles in a wet medium.	36
4.14. The specific wear rate of untreated and cryogenic treated AZ91 in a dry medium.	37
4.15. The specific wear rate of untreated and cryogenic treated AZ91 in a wet medium.	38
4.16. The specific wear rate of untreated and cryogenic treated AM60 in a dry medium.	39
4.17. The specific wear rate of untreated and cryogenic treated AM60 in a wet medium.	40
4.18. Coefficient of friction of untreated and cryogenic treated AZ91 in a dry medium.	41
4.19. Coefficient of friction of untreated and cryogenic treated AZ91 in a wet medium.	42
4.20. Coefficient of friction of untreated and cryogenic treated AM60 in a dry medium.	43
4.21. Coefficient of friction of untreated and cryogenic treated AM60 in a wet medium.	44

LIST OF TABLES

<u>Table</u>	<u>Page</u>
2.1. Some magnesium alloys used in automotive and aircraft (Avedesian and Baker 1999; Dziubińska et al., 2016).	6
2.2. Properties of magnesium alloys (Mert 2017).	9
2.3. Mechanical properties and chemical composition of magnesium alloys (Mert 2017).....	10
4.1. Data extracted from Tafel curves of untreated and treated AZ91 and AM60.	24

1. INTRODUCTION AND PURPOSE

Magnesium is the eighth-most abundant element on the Earth and one of the lightest of all light metals (34 % lighter than aluminum and 74 % lighter than steel). With the low density of 1.738 g/cm³, magnesium has attracted the attention of material and structural engineering scientists in recent years due to its great potential in engineering materials (Avedesian and Baker 1999; Bommala et al., 2019; Demir et al., 2014; Dieringa and Kainer 2007; Ding 2016; Ilanaganar and Anbuselvan 2018; Mert 2017). Despite its lightweight, it has high specific strength, high stiffness, good heat dissipation capacity, and good damping capacity and is readily available (important qualities, especially in applications where the material must be both lightweight and strong). Magnesium alloys are widely used in a variety of applications in a wide range of sectors from aerospace, medical, automobile, electronics, sports, and many other industries, especially if strong, lightweight material is needed (Esmaily et al., 2017; García-Rodríguez et al., 2017; Mao et al., 2017; Mert 2017).

Magnesium alloys in which aluminum and zinc carry a larger presence than the other alloying elements are a particular focus because of the part they play in improving the alloy in terms of mechanical strength, improved ductility in room temperature, and improved corrosion resistance. Aluminum is the most common alloying partner in Mg alloys, and zinc is the second-most common element in Mg alloys. In addition, AZ91 alloys are some of the most-used Mg alloys due to their good castability, ductility, and mechanical strength.

However, a high corrosion rate and rapid wear are major problems that hinder that use of the alloy in many engineering applications, especially in applications where saline is present (Akyüz 2019; Avedesian and Baker 1999; Chelliah et al., 2017; Chelliah et al., 2019; Hoche et al., 2007; Ilanaganar and Anbuselvan 2018; Klassen et al., 2005; Klassen et al., 2003; Mert 2017; Oteyaka et al., 2012b; Öteyaka et al., 2003). A limitation of the tribological use of magnesium alloys containing Al and Zn is due to the β -Mg₁₇Al₁₂ phase located in the grain boundaries, making the alloy brittle. To enhance the wear resistance, researchers investigated different methods, such as heat treatment (Maldar et al., 2010; Meshinchi Asl et al., 2010; Zafari

et al., 2014; Zheng et al., 2016) and reinforcing the matrix with ceramic particles (Aatthisugan et al., 2017; Chelliah et al., 2016; García-Rodríguez et al., 2017). Die-cast and homogenized AZ91 alloy were exhibited a higher coefficient of friction and lower wear rate because the eutectic phase acts as a barrier (Chelliah et al., 2017). On the other hand, the wear rate of hot rolled AZ31B was dependent on the applied load and sliding velocity. The main wear mechanisms of magnesium alloys were obtained abrasion, oxidation, delamination, and melting (Mert 2017). The effect of the alloying element on AZ91 was investigated and the AZ91 treated with Y using T6 showed better wear resistance due to large amounts of fine Mg₁₇Al₁₂ distributed in the grains (Yan and Wang 2016). Moreover, it was found that increasing the applied load decreases the coefficient of friction (COF) but increases the wear rate (Chelliah et al., 2017; Ilanaganar and Anbuselvan 2018; Mert 2017). AM60 alloys are one of those magnesium alloys that studies are being carried on as prospects of engineering materials. The AM60 is the combination of aluminum, manganese, and other alloying elements to form an alloy that has good mechanical strength, good ductility and is considerably more corrosion resistant than the pure magnesium (Jia et al., 2018).

Recently, the deep cryogenic treatment method attracted attention due to improving the corrosion and wear performance of the materials (Amini et al., 2014; Asl et al., 2009b; H. 2017). The cryogenic heat treatment is the means of exposing materials to temperatures as low as -190°C for a period, allowing the extremely cold conditions to alter the microstructure of the materials by reducing the residual stress in the material, improving the corrosion resistance, and enhancing the wear performance in some materials. The process has been conducted on steel and other materials, and the results have shown that the materials in question have registered significant improvement in their corrosion and wear resistance behaviors (Bhavar et al., 2015; Jiang et al., 2010a; Wang et al., 2012).

A few studies have been conducted on the wear behavior of cryogenically treated magnesium alloys. For example, deep cryogenic treated sample of AZ91 had a 16 % to 23 % better wear rate compared to untreated samples after a 1000-m sliding distance under the load of 600 g because of the fine distribution of precipitates (β) in the treated samples (Amini et al., 2014). On the other hand, it was obtained that the deep cryogenic treatment affected the wear

rate at higher loads ($>50\text{N}$). They explained that the wear was improved due to the new morphology of β particles (coarse divorced eutectic β phase) inserted into the matrix (Asl et al., 2009b). This modification of the microstructure after the cryogenic treatment of the AZ91 alloy was explained that the cryogenic treatment of the disordered solution changed to an ordered solution, resulting in a new superlattice structure in the AZ91 alloy (Liu et al., 2012). The wear properties of cryogenically treated AZ91 alloy had been investigated only in a dry environment and the soaking time did not exceed 24 h. Regarding to the literature, the wear properties below of 5 N and cryogenic treatment for 48 h was not studied. Moreover, it was seen that the isotonic solution (0.9 wt.% NaCl) was not investigated as wet medium for possible use of alloy as implant.

In this study, the wear properties of cryogenic treated AZ91 and AM60 magnesium alloy with a soaking time of 48 h were investigated in both dry and wet environments (0.9 wt.% NaCl) in comparison with the untreated AZ91 alloy. For this purpose, the alloy was submitted to deep cryogenic treatment ($-196\text{ }^{\circ}\text{C}$) for 48 h. The wear performance in dry and wet medium was tested using pin-on-disc method. The wear track, specific wear rate (SWR) and coefficient of friction (COF) of untreated and treated AZ91 alloys were investigated with using statistical analysis. On the other hand, the main goal of this research is to observe any improvement in corrosion resistance of a 48 h cryogenically treated AZ91 and AM60 alloy over a non-cryogenically treated AZ91 and AM60 sample, to give us some knowledge as to whether using the cryogenic means of treating the AZ91 and AM60 alloy helps in improving the materials corrosion resistance in the 0.9 % NaCl isotonic solution. For the above-mentioned purpose, all the electrochemical means of corrosion test such as; the open circuit potential (OCP), polarization, cyclic voltammetry (CV) and electrochemical impedance spectroscopy (EIS), were conducted on the samples.

2. LITERATURE REVIEW

2.1. Magnesium and its Alloys

Magnesium the eight most abundant element in the universe, was named after the city where it was first founded “Magnesia”, a district of Thessaly/Greece and was recognized as an element by Joseph Black in 1755. Abundant as it is, magnesium has never been found free, it is always tied within a compound with other elements in some case to form important minerals that include dolomite $\text{CaMg}(\text{CO}_3)_2$, magnesite MgCO_3 , kieserite $\text{MgSO}_4 \cdot \text{H}_2\text{O}$, and pyrope garnet $\text{Mg}_2\text{Al}_2(\text{SiO}_4)_3$ (Avedesian and Baker 1999). Magnesium and its compounds are formed from seawater, well and lake brines and bitterns, and form over 60 minerals; some of which are highlighted in the above sentence. The element was first isolated by Sir Humphry Davy (1778-1829) in the year 1808, who used electrolysis on a mixture of magnesia and mercuric oxide; close to 200 years after it had been first discovered. Michael Faraday, in the year 1833 obtained magnesium through the electrolysis of a fused anhydrous magnesium chloride, and in two decades later, Robert Bunsen created an electrolytic cell for the production of isolated magnesium, some years after that Bunsen’s electrolytic cell was modified to produce the light metal in a larger scale in Germany, and by the year 1909, the production of magnesium had seen improvement to a level of limited industrial production (Cardarelli 2013; Kramer 2001).

It took over a century following its isolation for the light metal to be in significant demand. The use of magnesium was mainly restricted to alloying with Aluminum alloys and to a lesser degree; for deoxidation process of steel, chemical and pyrotechnics (Botelho 2015) among other minor uses; as it was at the time not considered a valid structural material. Magnesium was first industrially produced in France by Caron and Deville in the year 1863 through the process of reducing a mixture of anhydrous magnesium chloride and calcium fluoride by sodium. The use of magnesium in a large scale generally began with German Air For, who use the metal in large quantities to produce fighter Aircraft part during both world wars (at a more extensive quantity during the second world war), the Americans also know to have used the light metal in some parts of their long-range bombers such as the B-52 and B-36 (Abbott et al., 2004) , the Soviet Union also used magnesium in their aircraft industry for the

production of TU-95 and TU-143 which had 1550 Kg and 780 Kg of magnesium respectively (Kumar et al., 2018).



Figure 2.1. Examples of application for magnesium alloys in Boeing 747: wing and seat components (Dziubińska et al., 2016).



Figure 2.2. Air conditioning system made of magnesium alloy WE43 for aircraft (Dziubińska et al., 2016).

After the second world war, the use of magnesium drastically reduced, the aviation industry also reduced the use of magnesium parts because they were perceived to be hazardous. However, the new coatings with fire retardants techniques allowed to reuse magnesium alloys in aviation industry (Dziubińska et al., 2016; Gloria et al., 2019). The magnesium alloys were used as gearbox, engine components, wings, fuselage skin, door, wheels, dashboard panels and seat components. The Figure 2.1 and Figure 2.2 shows some magnesium alloys used in Boeing 747 (Dziubińska et al., 2016). On the other hand, the Table 2.1 presents the alloy used in automotive and aerospace industry.

Table 2.1. Some magnesium alloys used in automotive and aircraft (Avedesian and Baker 1999; Dziubińska et al., 2016).

Company	Part	Model	Alloy
FORD	Clutch housing, oil pan, steering column	Ranger	AZ91B
GM	Valve cover, air cleaner	Corvette	AZ91D
Boeing	Seat	747	AZ91D
Alfa-Romeo	Miscellaneous components (45kg)	GTV	AZ91B
Toyota	Steering Wheel	Lexus	AM60B
Boeing	Compressor casing	747	WE43

Magnesium in its pure form does not have adequate mechanical properties to be used as an engineering material due to factors including its high reactivity and rapid corrosion rate in an open environment (especially when chlorine ions are present in the environment), as a result of which it's usually alloyed with other metals to form a material (magnesium alloy) that can be more useful in engineering application. The metals that can be chosen as an alloying element with magnesium are determined by the atomic size of the metal (the metal must have a fitting atomic size to the magnesium structure). the chemical affinity with silicon and tin (which cause the formation of a stable compound) and the relative valence effect are major parameters that limit the types of metals that could be alloyed with magnesium (Botelho 2015). Apart from iron and its chromium groups except for nickel, most common metals can form alloys with magnesium. Aluminum, calcium, copper, lithium, manganese, silicon, rare earth, zinc and zirconium are some of the most prominent elements that alloy with magnesium.

2.2. Properties of Magnesium

Magnesium, an alkaline metal (belonging to the group 2 of the periodic table) is the lightest regular metal used in structural engineering; with a density of 1.74 g/cm^3 in its solid state. Its atomic number is 12, atomic mass is 24, atomic diameter is 0.320 nm, it has one main oxidation state of (+2), and three naturally occurring isotopes (^{24}Mg , ^{25}Mg and ^{26}Mg), amongst which ^{24}Mg is the main isotope at 79 % of the total mass (Avedesian and Baker 1999).

Magnesium appears in a hexagonal close structure in its solid metallic state (Figure 2.3). Magnesium may be considered a perfect close hexagonal material because its c/a ratio of 1.623 (derived from its $a=0.320$ and $c=0.521$) is very close to the ideal values of hexagonal close structures which is 1.633 (Hu et al., 2018).

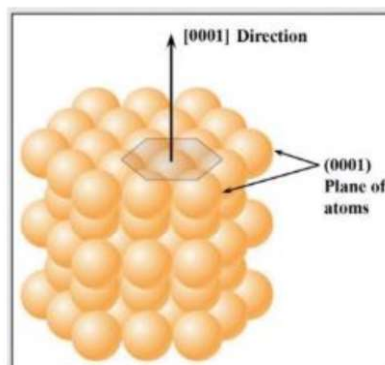


Figure 2.3. Magnesium hexagonal close-packed crystal structure (Callister and Rethwisch 2020).

The atomic diameter of magnesium (0.320 nm) is quite suitable for the dissolution of the atoms of the alloy elements, thus making it an element around which the packaging with other atoms is considered favorable from a physical metallurgical point of view (Hu et al., 2018). Magnesium has enough hardness to be used as a structural material for application that don't not include severe abrasion. The abrasion resistance among magnesium alloys only varies up to 20 %, even though the variation in hardness among magnesium alloy is quite wide.

Magnesium has a boiling point of $1107 \pm 10^\circ\text{C}$, it has a Heat of Combustion 25.1 MJ/kg, it has a heat of fusion for pure magnesium is 0.370 ± 0.015 MJ/kg. the addition of alloying element elements does not to a large extend affect the specific heat of fusion of magnesium. The element's thermal conductivity is slightly affected by temperature variations. Thermal conductivity is greatly affected by the Alloying. The coefficient of thermal expansion is also not affected to a large degree by the alloying. 2.96 - 4.20 percent liquid volume; is the amount of shrinkage that happens when pure magnesium transforms from liquid to solid, relative to the volume of the liquid metal.

2.3. Effect of Alloying Element on Magnesium

The properties of magnesium alloys depend on the alloying elements that are combined with the magnesium to form an alloy. This is mainly because different elements are known to have certain properties which if added to the magnesium alloy would lead to the magnesium alloy adopting those properties, thereby making it a better material in terms of those properties (Table 2.2).

Aluminum, known for its high mechanical strength, ductility, and good corrosion resistance is one of the major alloying partners with magnesium. Studies have shown that commercially based Mg alloys contain 3-13 % of aluminum (Abdelaziz et al., 2017). The alloying of aluminum with magnesium and other elements help create a magnesium alloy that is relatively mechanically stronger, more ductile at room temperature, and more corrosion resistant (Dunmade 2012). AZ92, AZ91, AZ63, AZ61, AZ31, AM60, and AM50 are some examples of the Mg-Al alloys in which aluminum holds a significant decent proportion of alloying element in the Mg alloy. Beryllium, an alloying element used in a little quantity (up to 0.001 wt. %) to help reduce the surface oxidation during melting, casting, and welding alloys. It's use in die-cast and wrought products quite easy and successful, however, in sand-casting it must be used judiciously because it coarsens the grain (C. Moosbrugger 2017). Calcium added to the magnesium alloy helps in raising the ignition point on the molten alloy significantly in the air (Tolnai et al., 2018). A thermally stable second phase; $Al_{12}Ca/Mg_2Ca$, can be attained with the addition of calcium in Mg alloy; helping suppress the forming of low melting point eutectic phase $Mg_{17}Al_{12}$ at the grain boundaries, which increases the elevated temperature strength and creep property incredibly (Sato and Seiji 1973). structural refinement and an increment in the mechanical properties would be attained with the addition of a small amount of calcium as an alloying element with mg alloys (Shengfa et al., 2006). Copper is another element noted for its hardness thus a study showing that the addition of a little amount of copper in AZ91 magnesium alloy increased the Tensile strength (UTS) of the alloys, an increase in the fluidity of the Mg alloy was also observed. Lithium known to be the lightest metal helps in reducing the density of mg alloys when added as an alloying element. It also increases the alloy's

ductility. A point to be noted is that Lithium could also reduce the alloys strength. Manganese is added to the magnesium alloy so that the iron (Fe) impurities which are a major cause of rapid corrosion are reduced thus making the alloy relatively more corrosion resistance. Manganese has a high electron affinity with Fe, therefore in Mg alloys containing Al, Fe is impounded by the formation of an intermetallic compound with Al and Mn - in the general form of an $Al_xMn_yFe_z$ compound decreasing corrosion rates dramatically (Esmaily et al., 2017).

Table 2.2. Properties of magnesium alloys (Mert 2017).

Alloy	Characteristics
AZ63A-T6	Good room-temperature strength, ductility, and toughness
AZ91C and E-T6	General-purpose alloy, moderate strength
EZ33A-T5	Good castability and damping capacity, pressure tight, creep resistant to 245°C (475°F)
WE43A-T6	High strength at room and elevated temperatures (to 290°C, or 550°F), good corrosion resistance
ZK51A-T5	Good room temperature strength and ductility
AM20-F	High ductility and impact strength
AM50A-F	Excellent ductility and energy-absorbing properties
AM60A	Similar to AM50A-F, but slightly higher strength
AZ91A, B	Excellent castability, good strength

The chemical composition and mechanical performance of some magnesium alloys are given at Table 2.3. Rare earth metals increase corrosion resistance, strength, and high-temperature creep in magnesium alloys. They help in improving castability by narrowing the freezing range of the Mg alloys, which reduces porosity. Zinc, an element that is second to aluminum as the most efficient and frequently used as an alloying element to Mg alloys helps improve the material's strength at room temperature and ductility simultaneously. It can increase corrosion resistance when added to magnesium alloys with nickel and iron impurities. It can

also produce precipitation-hardenable alloys with good strength when combined with zirconium and rare earth metals as alloying elements in mg alloys (Avedesian and Baker 1999).

Table 2.3. Mechanical properties and chemical composition of magnesium alloys (Mert 2017).

Alloy	Composition (%)						Tensile Strength	Yield Strength			Hardness
	Al	Mn	Th	Zn	Zr	Other	(MPa)	Tensile (MPa)	Compressive (MPa)	Bearing (MPa)	(HB)
AZ92A-T6	9.0	0.1	--	2.0	--	---	275	150	150	450	84
EZ33A-T5	--	--	--	2.7	0.6	3.3 RE	160	110	110	275	50
AZ63A-T6	6.0	0.15	--	3.0	---	---	275	130	130	360	73
AZ91C and E-T6	8.7	0.13	--	0.7	---	---	275	145	145	360	66
ZE63A-T6	--	--	--	5.8	0.7	2.6 RE	300	190	195	---	60-85
ZK61A-T5	--	--	--	6.0	0.7	---	310	185	185	---	58
ZK61A-T6	--	--	--	6.0	0.7	---	310	195	195	---	70

2.4. Cryogenic Treatment

The cryogenic treatment that modifies the microstructure of materials is an ancient technique. It allows to enhance the microstructure and mechanical properties of materials (Figure 2.4). The atoms organization in the materials change from disordered to ordered form (Figure 2.5). Basically, the material is gradually heated from room temperature to the sub-zero temperature. This method uses both types of process; shallow (-80 °C) and deep (-196 °C) cryogenic temperatures.

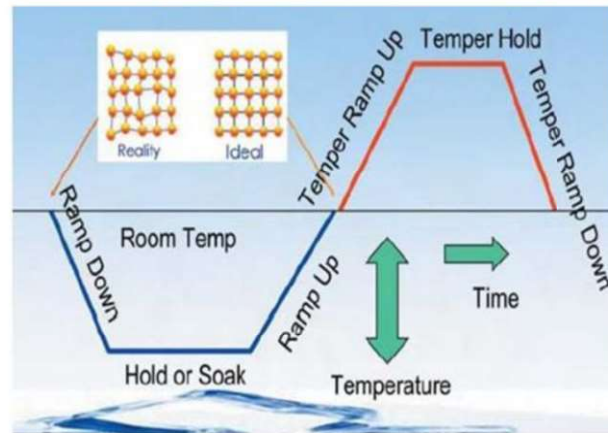


Figure 2.4 General cycle of cryogenic treatment (Sonar et al., 2018).

After a span of time at these temperatures, the material is warmed slowly to room temperature. In this method, gaseous Nitrogen was used to avoid thermal stress. Preciado et al. (Preciado et al., 2006) employed on quenched steels to finish the martensite transformation and precipitate residual austenite. The cutting tools technology also use this treatment successfully; the cost of cutting tools reduced by half using deep cryogenic treatment (Mohan Lal et al., 2001). Moreover, the technique is used in different industry such as automotive, aerospace, medical applications (Sonar et al., 2018).

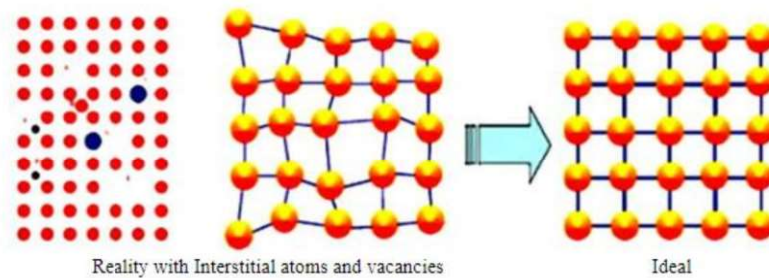


Figure 2.5 Modification of the atom structure (Sonar et al., 2018).

2.5. Corrosion Behaviour of Magnesium Alloys

The corrosion of magnesium is well studied in the literature (Klassen et al., 2005; Klassen et al., 2003; Öteyaka et al., 2012a; Öteyaka et al., 2012b; Öteyaka 2002; Öteyaka et al., 2003). The corrosion resistance of magnesium alloys depends of many factors such as alloying element, manufacturing process and heat treatment. All these parameters affect the microstructure of the material that play a critical role on corrosion. Among metallurgical factors, for example higher content of iron increase the corrosion rate (Öteyaka 2002). On the other hand, the influence of nickel on magnesium, magnesium-manganese and magnesium-zinc was well studied and demonstrated (Friedrich and Mordike 2006). In general corrosion, the magnesium was susceptible to galvanic corrosion while in localized corrosion they are more prone to pitting corrosion, crevice corrosion and filiform corrosion. It is well cited that magnesium has -2.30 V at 25°C with respect to the hydrogen electrode potential taken as zero. In general, the MgO film shows a respectable surface protection in rural and some industrial environments (Avedesian and Baker 1999). It was found that the magnesium alloys were susceptible to pitting corrosion at the presence of Cl^- ions. For this reason, it is well important to investigate the corrosion of magnesium alloys when it is used in marine atmosphere. It was reported by Öteyaka et al. that the in the solution containing chloride ions, the corrosion potential (E_{corr}) of the AZ is less active than ZA group but the E_{corr} of AZ group is more active than ZA group in solutions without Cl^- ions (Öteyaka 2002). Moreover, SRET (Scanning Reference Electrode Technique) technique showed that pitting corrosion occurred less frequently on AZ alloys than the ZA alloys (Figure 2.6) (Klassen et al., 2005). The black color shows the pitting area (anode) while the rest zone had cathodic behaviour.

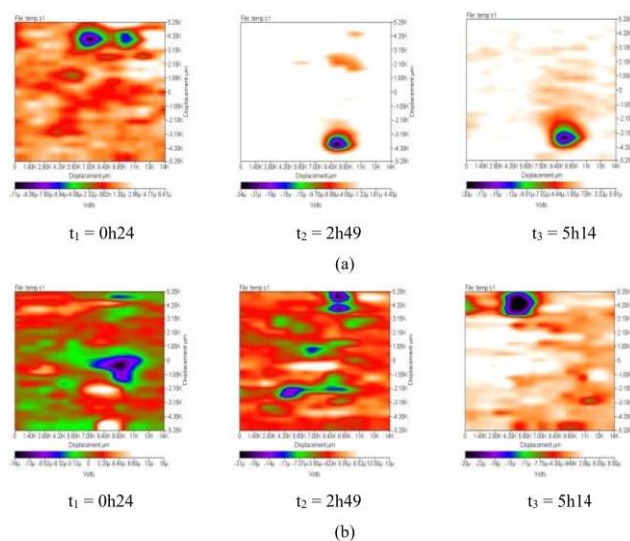


Figure 2.6. SRET maps for a) AZ91E and b) ZACS1040305 in 5% NaCl solution saturated with $Mg(OH)_2$ at $pH = 9$ and $25^\circ C$ for 3 different time periods (Klassen et al., 2005).

The corrosion potential of AZ91E and ZAC10403 was evaluated by Öteyaka et al. (Öteyaka et al., 2003) and they found that AZ91E had E_{corr} around -1.31 V nobler than ZAC10403 and ZACS1040305. On the other hand, it was observed for both alloy localized corrosion on their surface and it was more pronounced for ZAC10403 (Figure 2.7).

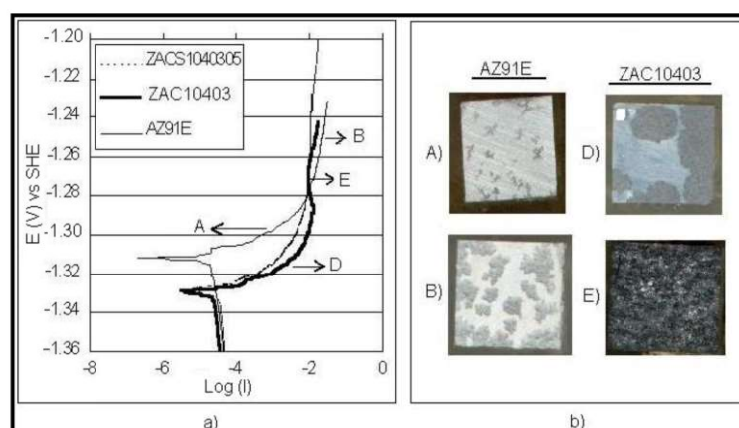


Figure 2.7. a) potentiodynamic behaviour of the AZ91E and ZAC10403 alloys in the 5% NaCl solution saturated with $Mg(OH)_2$ at $pH = 9$ and $25^\circ C$; b) Corroded surface of AZ91E and ZAC10403 (Öteyaka et al., 2003).

2.6. Wear Behaviour of Magnesium Alloys

Different wear type was seen on magnesium alloys such as abrasion, delamination, oxidation and adhesion. The wear performance of magnesium alloys depends on counterface materials, surface finishing, microstructure as well as tribometer parameters (Figure 2.8). The effect of microstructure was studied by Liu et al. (Liu et al., 2012). They stated that after cryogenic treatment, the disordered solution was changed to ordered solution for AZ91 alloy. In addition, they observed twins after 10 h of DC treatment of AZ91. This twin formation after DC treatment was also observed by different works (Amini et al., 2014; Asl et al., 2009a; Jiang et al., 2010b; Liu et al., 2012).

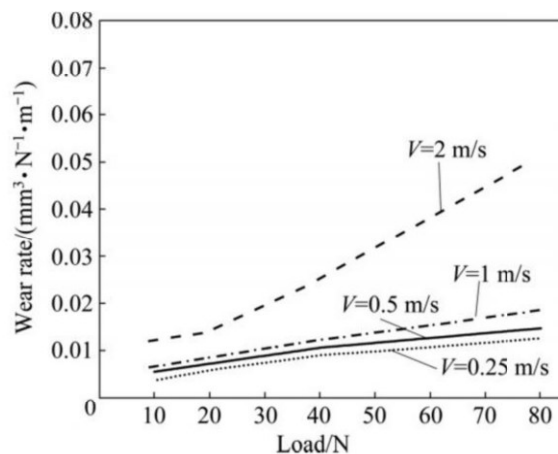


Figure 2.8. The influence of load on the hot rolled AZ31 alloy with different velocity (Mert 2017).

However, there is no deep literature analysis on twin formation mechanism. On the other hand, Asl et al. (Asl et al., 2009a) effectuated a dry sliding wear test on DC-treated AZ91 and they found that it had superior wear resistance compared to untreated AZ91. They also mentioned that DC treatment lead two types of β phase and both phases after DC treatment played a major role on the wear behavior.

The wear behavior of DC treatment was addressed by different studies. For example, Chelliah et al. (Chelliah et al., 2017) tested wear behavior of die cast and homogenized (T4) AZ91 using a pin-on-disc in dry condition. They pointed out that die-cast AZ91 versus homogenized AZ91 had lower coefficient of friction (COF) versus higher wear rate. They also stated that delamination mechanism was the predominant wear mechanism of AZ91 alloys. The quench environment effect was investigated by Amini and al. (Amini et al., 2014). They reported that the cooling rate greatly influenced hardness and increasing the cooling rate had a positive impact on the hardness of AZ91. In another study, both samples - solution heat-treated AZ91 and age hardened AZ91 alloy - were submitted to against steel AISI 250 using the pin-on-disc method. They showed that solution heat-treated AZ91 had a lower specific wear rate compared to age-hardened AZ91 (Kumar et al., 2015). Yan et al. (Yan and Wang 2016) reported wear properties of extruded AZ91 alloy treated with yttrium. They described that abrasion, oxidation, delamination and plastic deformation wear mechanisms were observed after a dry sliding test. In addition, AZ91 treated with yttrium showed better wear resistance by solution treatment and following T6 heat treatment. Similar findings were noted by like Li and Jiang (Li and Jiang 2011), Li et al. (Li et al., 2013), and Amini et al. (Amini et al., 2014) on the effects of DC treatment on the properties of magnesium alloys.

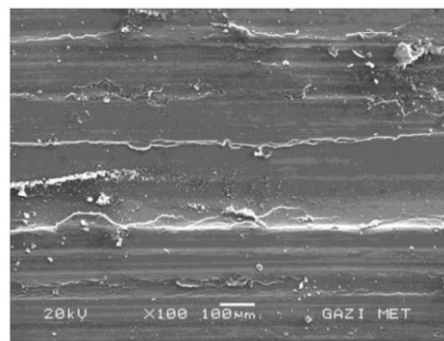


Figure 2.9. SEM images showing the delamination of hot rolled AZ31 after at load 40 N and velocity of 1 m/s (Mert 2017).

3. MATERIALS AND METHODS

3.1. Materials Preparation

The magnesium alloy AZ91 and AM60 used in this experiment was acquired by the firm Varzone Ltd. in solid state having a dimension of 300x200x300 mm with a chemical composition given at (Table 3.1). The chemical composition of AZ91 and AM60 in wt. (%). From the solid, cubes with a dimension of 10x10x10 mm were cut to prepare the surface area of 1 cm² and microstructure analysis. The samples were divided into two groups and classified as; (i) “to be cryogenically treated” and (ii). “not to be cryogenically treated”.

Table 3.1. The chemical composition of AZ91 and AM60 in wt. %.

Alloy	Alloying Elements (wt. %)			
	Al	Mn	Zn	Mg
AM60	6.26	0.29	0.1	Bal.
AZ91	8.7	0.25	0.65	Bal.

3.2. Cryogenic Treatment

The samples that were to be cryogenically treated were placed in a special box at room temperature to be exposed to cryogenic treatment (Figure 3.1). The temperature in the room was then gradually reduced at the velocity of 5°C/ min to -196 °C and the samples were left there for 48 h, then the temperature in the room was gradually regulated to room temperature. The samples were then relabeled as AZ91 cryogenic treated, AM60 cryogenic treated, AZ91 untreated and AM60 untreated. Afterward, the specimens were each ground with an 800 and 1200 grinding paper and cleaned with alcohol followed by distilled water before each experiment.



Figure 3.1. Cryogenic treatment setup.

3.3. Electrochemical Test

A standard three-electrode cell system was used in this investigation (Figure 3.2). The alloys with a surface area of 1cm^2 was used as the working electrodes, a standard silver chloride electrode as the reference electrode, and graphite rod was used as the counter electrode. The corrosion test was conducted in a 1 L isotonic serum (0.9 wt. % NaCl solution). With the help of potentiostat Gammry Interface 1000, the data obtained from the experiment were then analyzed by a Gammry Echem analysis software. The electrochemical methods of corrosion test (the potentiodynamic polarization, the cyclic voltammetry, the open circuit potential (OCP) measurement, and the electrochemical impedance spectroscopy (EIS) measurement were all employed in this study. The OCP was conducted for 2 h and E_{corr} vs time was recorded. The potentiodynamic test was apprehended between -2 mV and $+0.5\text{ mV}$ at the velocity of 5 mV/s .

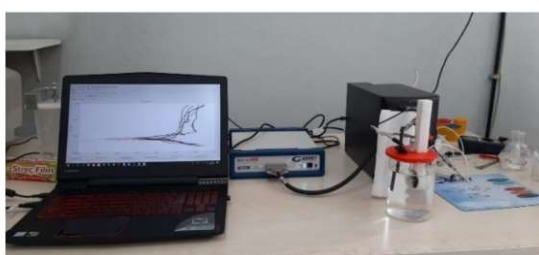


Figure 3.2. Electrochemical setup.

The cyclic voltammetry (CV) was used at a scan rate of 100 mV/s to understand the kinetics of the corrosion. EIS was performed in the range of 100 kHz - $0,01\text{ kHz}$ and each experiment was repeated 3 times. An optic microscope (Nikon model) was used to take the

images of the samples at the magnification of X500. Before imaging, the samples were ground with a 1200 grit grinding paper and polished with 1 μ m diamond and surface was finally etched by picral reagent.

3.4. Wear Test

The wear performance of the materials was tested using a tribology machine pin-on-disc (CSM tribometer). A steel ball was used as the contact material to help inflict wear on the material (Figure 3.3). Different weighted disks of 1 N, 3 N, and 5 N served as the load on the steel ball to inflict different degrees of wear on both samples. The sliding velocity of 0.5 cm/s was set for all tests. This helped in the comparisons regarding which group of samples performed better than the others regarding how much they were affected by the wear inflicted on them. The experiments were conducted in dry and wet media. The only difference in how the test was conducted in the different media was the housing used to hold the material fastened to the tribometer machine to allow a steady flow of the housing that holds the steel ball for a uniform sliding of the ball on the sample so that the wear process can happen in a smooth fashion. The wet medium required housing that hosts the sample and 0.9 wt.% NaCl solutions that the sample soaked in to ensure that the experiment was done in a liquid solution. A profilometer meter Mitutoyo SJ-401 was used to measure and provide the required data of the experiment. A Nikon model optical microscope was used to take the images of the samples that have undergone the test process at a magnification of 100x.



Figure 3.3. Wear setup.

4. RESULTS AND DISCUSSIONS

4.1. Effect of Treatment on the Microstructure

The microstructure of AZ91 alloy before and after it underwent cryogenic treatment is displayed in the as Figure 4.1 a-b, respectively. In the first image Figure 4.1a, the untreated sample is seen to exhibit two different phases, a scattered β phases which are surrounded by a lamellar eutectic ($\alpha + \beta$) phase (dark black). The β -phase aluminum-rich compared to the surrounding Mg-matrix (white color) in Figure 4.1a. This microstructure is consistent with work elsewhere [26]. The form of β phases in the microstructure has seen drastic transformation after the cryogenic treatment, the eutectic phase can be seen to be less intense around the β -phase, it can also be observed that the eutectic phase has penetrated in the matrix. In addition, twinning was observed in the morphology due to cryogenic treatment. This microstructural transformation accounts for the improvement of the mechanical properties of the treated sample when compared to the untreated sample. The penetration of the eutectic phase to the matrix also brings about the spread of aluminum to the matrix which could lead to a better corrosion performance in the material.

The modification on the microstructure of AM60 after cryogenic treatment was exhibited at Figure 4.1c-d. At first glance, untreated AM60 had scattered β phases confined with eutectic ($\alpha+\beta$) phases (dark black) in the Mg-matrix (white color) (Figure 4.1c). After DC treatment, the microstructure change drastically; the eutectic phase was less intense around β phases and interestingly twinning was observed at some places with different magnitude (Figure 4.1d). It was described by the literature that β phases play a major role in the corrosion of magnesium alloy. In this case, twins can affect the corrosion behavior beside of β phases.

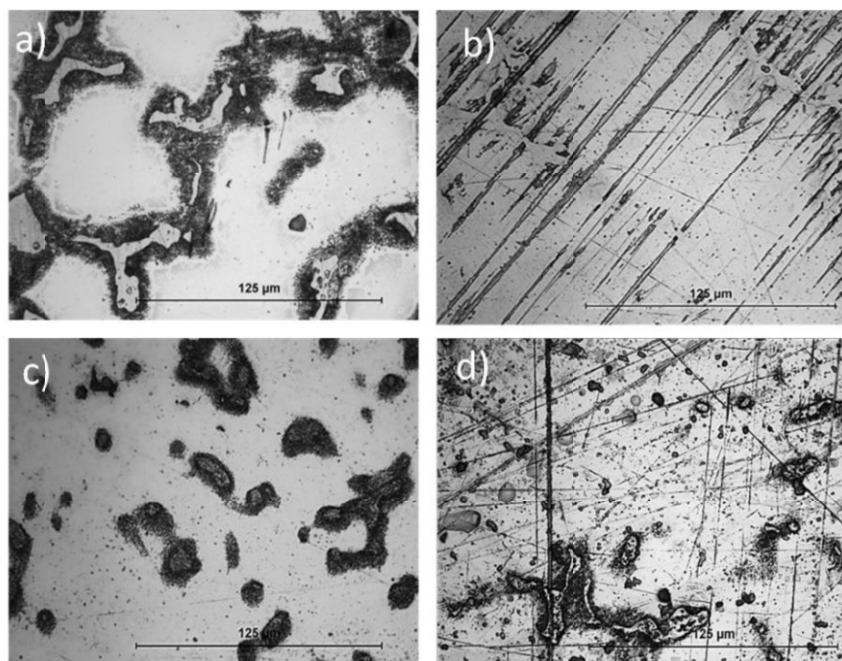


Figure 4.1. Optic images of AZ91 and AM60 at magnification of x500; a) AZ91 untreated b) AZ91 cryogenic treated c) AM60 untreated d) AM60 cryogenic treated.

4.2. Electrochemical Results

4.2.1. Open circuit potential (OCP)

Figure 4.2 exhibits the results of the OCP measurement of the treated and untreated samples of AZ91 in the isotonic solution. The untreated sample recorded an E_{corr} of -1.57 V and -1.54 V for the starting and the ending of the 2 h they were immersed in the isotonic solution, respectively. It also recorded curves similar to that which was recorded in the evaluation of AZ91 in diluted 3.5 wt %NaCl solution. While the E_{corr} of the treated sample had a similar behavior but after 45 min. of immersion it had superior corrosion resistance compared to the former. The untreated sample showed a better corrosion resistance performance from the beginning of the experiment, until around the 15 min. in the experiment when the treated sample gains corrosion resistance superiority for about 10 min. After which the untreated sample regains the edge over the rival sample for another 20 min. (45 min. in the test). However,

towards the 47th min. into the test, the treated sample edged and maintained the corrosion resistance superiority until the end of the 2 h test. With the overall comparison, it could be seen that the treated sample had an E_{corr} superiority for over 78.8 % of the immerse time in the isotonic saline solution while the untreated sample only managed to be more corrosion resistance for less than 21.2 % of the total immerse time. This goes to show that the cryogenic sample would have a better performance in a corrosive environment compared to the rival sample, as far as this result are a concern.

The open circuit potential of treated and untreated AM60 started at -1.54 V after immersion in the saline solution and it completed around -1.52 V after 2 h (Figure 4.2). However, DC treated AM60 began more cathodic (-1.58 V) but it finished at a slightly more anodic (-1.51 V) compared to untreated AM60. The analysis of E_{corr} /time behavior of samples also demonstrated that untreated AM60 had superior corrosion resistance for the first 1h the samples were imersed in the isotonic solution and throught out the next hour of imersion time, the treated sample was seen to show more relatively more corrosion resistance values than the untreated sample. The overall performance of both samples would be hard to compare from this test as one was seen to be superior for 1 h and the other takeover for the other 1 h of the overall test time.

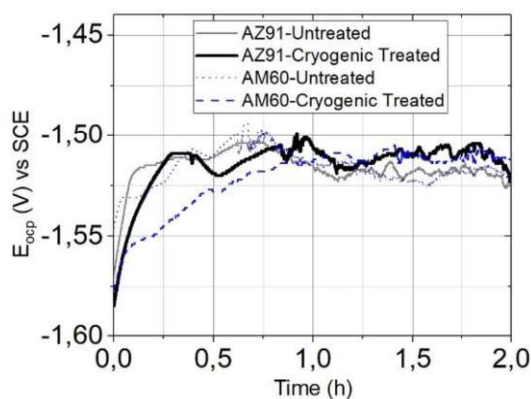


Figure 4.2. The E_{corr} /time plots of untreated and treated of AZ91 and AM60 in isotonic solution.

4.2.2. Potentiodynamic and cyclic voltammetry

Based on the results shown by Figure 4.3, it can be observed that the AZ91-cryogenic treated sample showed a more notable passivation behavior than the compared sample, giving a more steep slope at the passivation zone. The passivation potential is an indicator of the material trying to protect itself from getting corroded by creating a protective film around the region attacked. The steeper the slope at the passivation region, the more resistance the material was able to make in dithering corrosion. At the end of the passivation potential also indicates the beginning of the pitting corrosion (E_{pit}) as well as the beginning of the corrosion products passivation of the pit. The minimal passivation showed by the untreated sample tells us that the treated sample has a more superior resistance quality to pitting corrosion, thereby would be able to survive deformation relatively longer.

Table 4.1 shows the E_{corr} , i_{corr} , E_{pit} , β_a , and β_c , values extracted from the Tafel curves in Figure 4.3. Polarization curves of the untreated and treated AZ91 and AM60 alloys in the isotonic solution (scan rate 5 mV/s). Both samples exhibited approximately similar E_{corr} value of -1.40 V, however the treated sample showed a relatively lower i_{corr} value of 377 μA while the untreated sample showed a higher i_{corr} value of 737 μA , further showing that the rate of oxygen dissolution was more rapid in the untreated sample which is a sign of less corrosion resistance. The E_{pit} values when looked at were found to be more favorable to the treated sample which shows a value of -1.25 V while the untreated sample showed a relatively lower E_{pit} value of -1.40 V, which indicates that the untreated sample was more prone to pitting corrosion compared to the rival sample. Cyclic voltammetry plots of the untreated and treated AZ91 alloys in isotonic solution were presented in Figure 4.4. The experiment confirmed that the untreated alloy had higher peak anodic current compared to treated alloy as found in Figure 4.4.

Results obtain from the potentiodynamic and cyclic voltammetry (CV) test are shown by Figure 4.3 and Figure 4.4. It can be observed that both samples have a similar pattern in how their curves look like, throughout the test, both showing some passivation behaviors in similar steepness in the slopes of the passivation curves. However, it can also be seen that the AM60

cryogenic treated sample continues with the passivation behavior slightly after the untreated samples is seen to have been overcome by the corrosion attack. The steeper the slope at the passivation region, the more resistance the material was able to make in dithering corrosion. At the end of the passivation potential also indicates the beginning of the pitting corrosion (E_{pit}) as well as the beginning of the corrosion products passivation of the pit. The results shown in this test tells us that corrosion behaviors of the two materials that were featured in the test are actually very close, with the cryogenic treated sample holding a very slight edge over the untreated sample as far as corrosion resistance is concern.

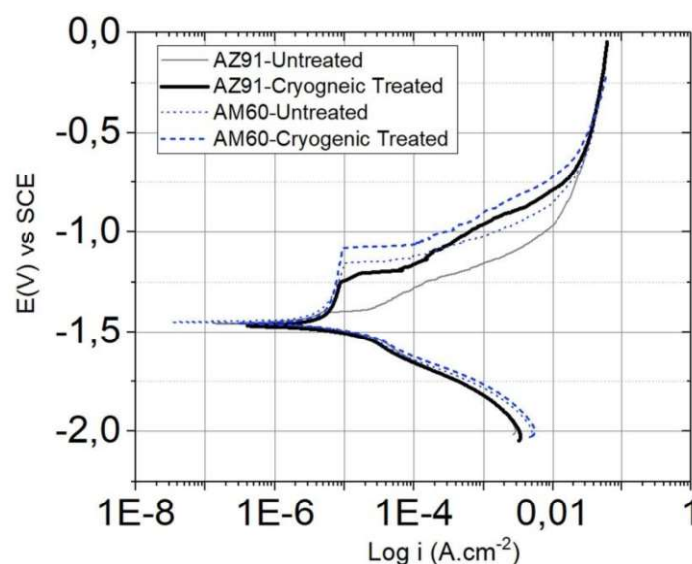


Figure 4.3. Polarization curves of the untreated and treated AZ91 and AM60 alloys in the isotonic solution (scan rate 5 mV/s).

Table 4.1. Data extracted from Tafel curves of untreated and treated AZ91 and AM60.

Samples	E_{corr} (V) vs. SCE	I_{corr} ($\mu\text{A}\cdot\text{cm}^{-2}$)	E_{pit} (V)	β_a (V/decade)	β_c (V/decade)
Untreated AZ91	-1,40	737	-1,40	$552.0e^{-3}$	$1,000e^{15}$
DC treated AZ91	-1,40	377	-1,25	$556.0e^{-3}$	$1,000e^{12}$
Untreated AM60	-1.44	23.70	-1.15	$229.8e^{-3}$	$227.9e^{-3}$
DC treated AM60	-1.43	30.00	-1.07	$350.9e^{-3}$	$233.4e^{-3}$

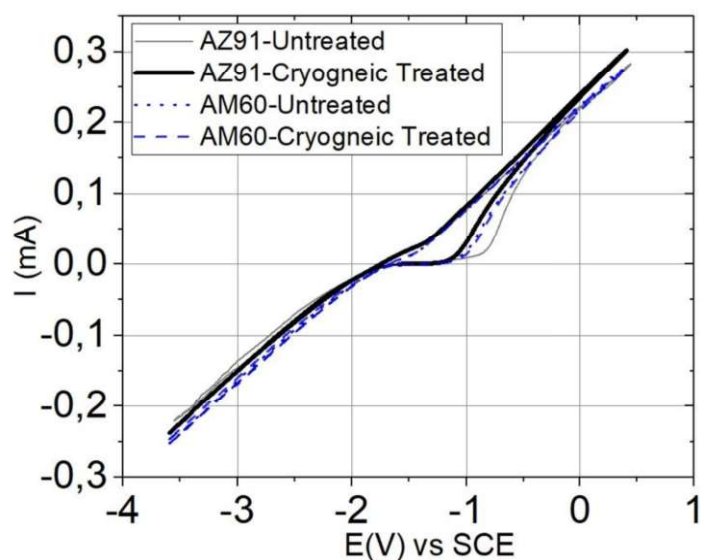


Figure 4.4. The cyclic voltammetry behavior of cryogenic-treated and non-treated AZ91 and AM60 alloys in the isotonic solution.

4.2.3. Electrochemical impedance spectroscopy (EIS) analysis

The EIS method was made to determine the influence of cryogenic heat treatment on the corrosion behavior of the AZ91 alloy in 0.9 wt. % NaCl solution. The Nyquist plots of the untreated and treated AZ91 samples are shown in Figure 4.5. The Nyquist plot illustrates the

corrosion resistance of the sample is directly proportional to the diameter of the semi-circle capacitive loop. As we can see in Figure 4.5, the Nyquist plots show two semicircles of different diameters, represent the different samples that were featured in the experiment. The treated sample is seen to have a relatively larger diameter, which is an indication of its relatively higher corrosion resistance. This is probably due to the modification of the microstructure that it decreased the galvanic corrosion between phases in the alloy.

The Nyquist plots of the results obtained from the test of the untreated and treated AM60 samples are revealed in Figure 4.5. The Nyquist plot demonstrates that corrosion resistance of the sample is directly proportional to the diameter of the semi-circle capacitive loop (Nyquist). As can be seen in the Figure 4.5, the two semicircles of slightly different diameters featured in the Nyquist plots represent the treated and untreated sample in the isotonic saline solution. From the curves showed we can see that the cryogenic treated sample has a relatively larger diameter, which if connect with the characteristic of nyquist plots will reveal to us that the untreated sample again shows corrosion resistance superiority relative to the untreated sample in this test.

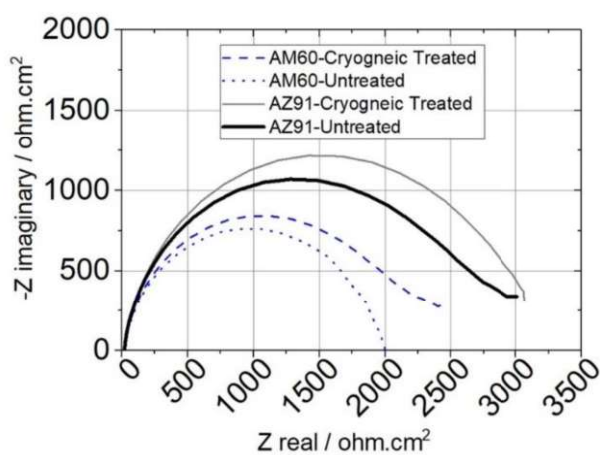


Figure 4.5. Nyquist plot of the untreated and cryogenic treated Az91 and AM60 alloys in an isotonic solution.

This we believe, is as a result of the microstructural transformation that cryogenic heat treatment has induced on the sample, decreasing the galvanic corrosion between the phases in

the alloy, thus making it a slightly more corrosion resistant than the untreated sample. The treated sample is seen to have a relatively larger diameter, which is an indication of its relatively higher corrosion resistance.

4.3. Wear Test Results

4.3.1. Optic microscope images of worn surfaces

In our previous studies (Gassama and Öteyaka 2019), the microstructures of the untreated and cryogenically treated AZ91 were investigated in depth. The microstructure of untreated AZ91 was composed of α -Mg and $\alpha+\beta$ phase rich in Al with a surrounding eutectic ($\alpha+\beta$) phase. The cryogenic treatment decreased the intensity of the eutectic phase around the β phase, and this twin phase was observed. Figure 4.6 and Figure 4.7 show the images obtained for a pin-on-disc wear assessment of untreated and cryogenically treated AZ91 samples. The different tests were conducted in both dry and wet media to determine the effects of the cryogenic treatment on the samples. The images show different types of wear that the samples endured during the test. The two different samples underwent the test procedures under similar conditions for the consistent comparison of the results. Some differences were observed in the effects of the experiment on the two different samples characterized in this work. One of the major differences is the difference in the width of their various wear tracts. Despite undergoing the process under the same load, this difference could be associated with the level of penetration the sample has allowed the steel ball to inflict on it. Because the ball is round, increased penetration was endured by the sample results in a wider wear track, and the level of penetration that the steel ball imposed on the sample could be related to the hardness of the sample. The harder the sample, the less penetration it would endure. Therefore, the sample with the lower wear track width is considered the more wear-resistant of the two samples.

Figure 4.6 is the image obtained from the pin-on-disc wear test on samples of cryogenically treated and untreated AZ91 magnesium alloys in a dry medium. At first glance, in plastic deformation, the delamination and abrasion mechanisms were observed for all samples by (Chelliah et al., 2017; Ilanaganar and Anbuselvan 2018; Zafari et al., 2014). When the

samples were tested under a 1 N load, the treated sample registered a wear track width of $309.5 \mu\text{m}^2$, while the untreated sample registered a wear track width of $299.6 \mu\text{m}^2$, which are values that are very similar. This shows that the cryogenically treated sample did not have any positive effects on improving the wear performance of the sample in the 1 N load category. For the load category of 3 N, the treated sample exhibited a wear track width of $363.6 \mu\text{m}^2$, while the untreated sample showed a wear track width of $361.8 \mu\text{m}^2$. The differences in the two values for the 3 N loads are almost insignificant, again showing the lack of effect of the cryogenic treatment on the materials in the wear performance under this load category. When the samples were subjected to testing under a load of 5 N, the observations showed a wear track width of $482.9 \mu\text{m}^2$ and $434.4 \mu\text{m}^2$ for the treated and untreated samples, respectively.

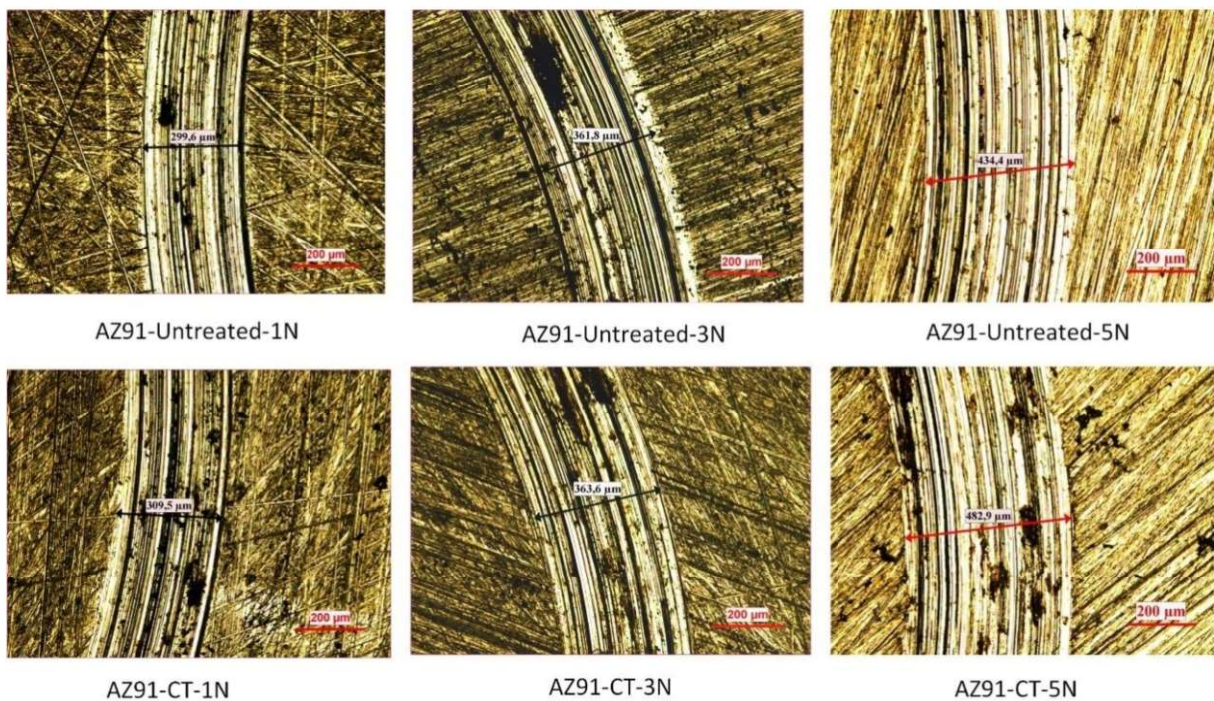


Figure 4.6. Worn surfaces of untreated and cryogenic treated AZ91 wear tracks in a dry medium.

The difference in the width of the wear tracks in the 5 N weight call are a little wider than the previous load classes tested, which again suggests that the cryogenically treated sample did not have a major positive influence on enhancing the wear performance of the samples under

investigation in the dry medium but also suggests that, as the load on the ball increases, the wear performance of the treated sample becomes better than the untreated sample, which is a result similar to that found by (Yan and Wang 2016).

Figure 4.7 shows images of the treated and untreated samples of AZ91 magnesium alloys tested in the 0.9 wt.% NaCl solution. At first glance, the wear tracks of the wet medium were not as prominent as the dry medium. Moreover, a higher amount of corrosion was observed due to the attack of Cl⁻ ions on the alloy during sliding. The samples visibly underwent different forms of wear abrasion and corrosion, which were the most notable among the types of wear endured by the samples under testing. Like the test conducted in the dry medium, different load categories are put on the sample to test the wear tolerance and to make comparisons between the cryogenically treated sample and the untreated sample to determine the effect of the cryogenic treatment on the wear performance of the material in question. Like the dry medium, the load categories of 1 N, 3 N, and 5 N were used in this test. When the 1 N load was applied on the samples, the wear track width values of 432.6 μm^2 and 434.3 μm^2 were observed for untreated and treated samples, respectively, showing that the treated sample had a slightly better wear resistance performance in the wet medium.

When the load of 3 N was applied to the samples, the samples were observed to show a wear track width of 511.5 μm^2 and 524.1 μm^2 for treated and untreated samples, respectively. Testing under the 3 N load also saw a slightly better wear resistance performance for the treated sample compared to the untreated sample in the wet medium.

The experiments conducted under the 5 N load produced the wear track width values of 554.6 μm^2 and 553.4 μm^2 for the untreated and treated samples, respectively. This load class saw a slightly different pattern, as the untreated sample has almost the same value as the treated value, suggesting that the cryogenic heat treatment has no visible positive enhancement on the material under investigation. The treated sample has been observed to generally have less corrosion on the wear tracks than the untreated samples, which is an indication that the cryogenic

treatment of the materials could help in their corrosion performance. Moreover, the optic microscope images have shown the sample to be less affected by wear than in the wet medium.

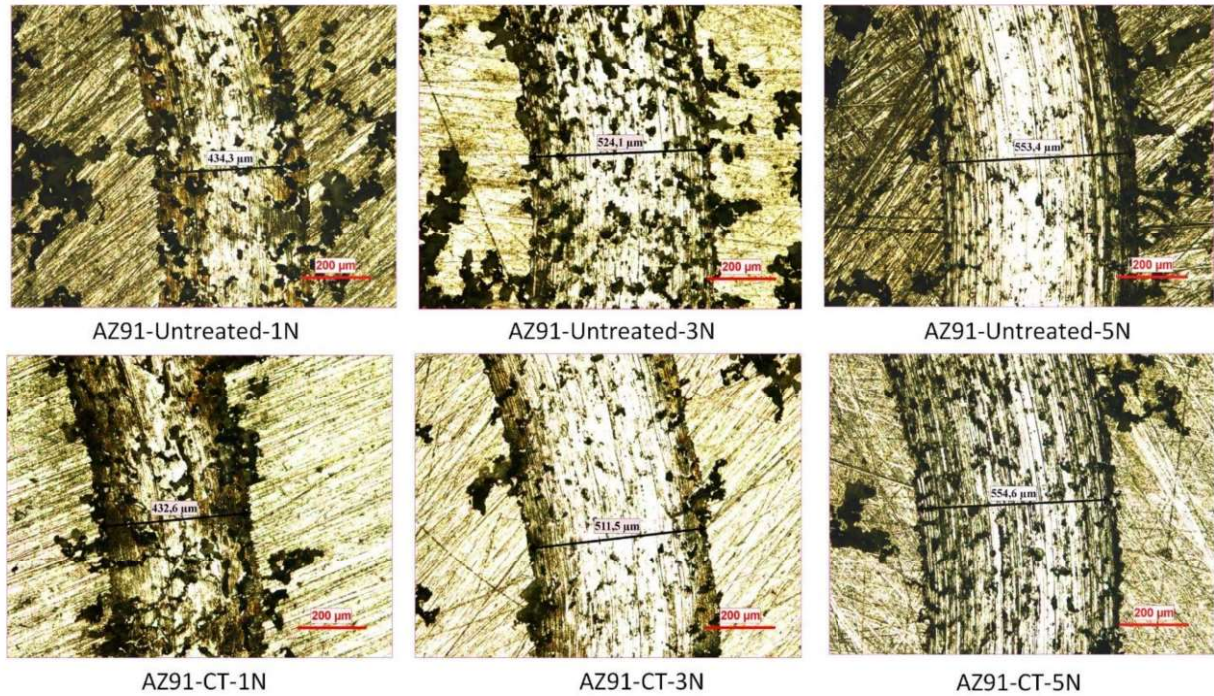


Figure 4.7. Worn surfaces of untreated and cryogenic treated AZ91 wear tracks in a wet medium.

Figure 4.8 is a microscopic image of the wear track of the untreated and cryogenic treated samples that were tested in a dry medium. the wear width for the treated and untreated sample when a load of 1 N was exerted on the ball were 324.4 μm and 302.3 μm respectively, with the treated sample having 22.1 μm less wear track width. When the load of 3 N was used in the experiment, a were track width of 363.6 μm and 328.8 μm were recorded for the untreated and treated samples respectively, with the treated sample showing a 34.8 μm less wear track width than the untreated sample. And finally, when the samples were subjected to the 5 N load, the values of 494.9 μm and 447.5 μm were registered as the wear track width for the untreated and treated samples respectively, with the treated sample showing a 50.4 μm less wear track width than the rival sample. For the wear track width values we can see that the width of the wear track consistently increases with the increased in load, this is simply because the more load exerted on the samples, the more penetration the steel-ball would induce on the samples, thus

increasing the width of the wear track as the surface area of the ball that interacts with the sample increases with the depth of penetration. However, samples that bear the same load and with whom all other test conditions remain constant, the only explanation that could be provided for the difference in their wear track width values is the impact of the cryogenic treatment on the sample. We have seen that in all the load categories from 1 N, 3 N, and 5 N the treated sample has consistently shown better values regarding the width of their wear track in the context of good wear resistance. We have also seen that the values get better as the load was increased on the sample further revealing the effective nature of the cryogenic treatment on enhancing the wear properties of the sample in a dry medium.

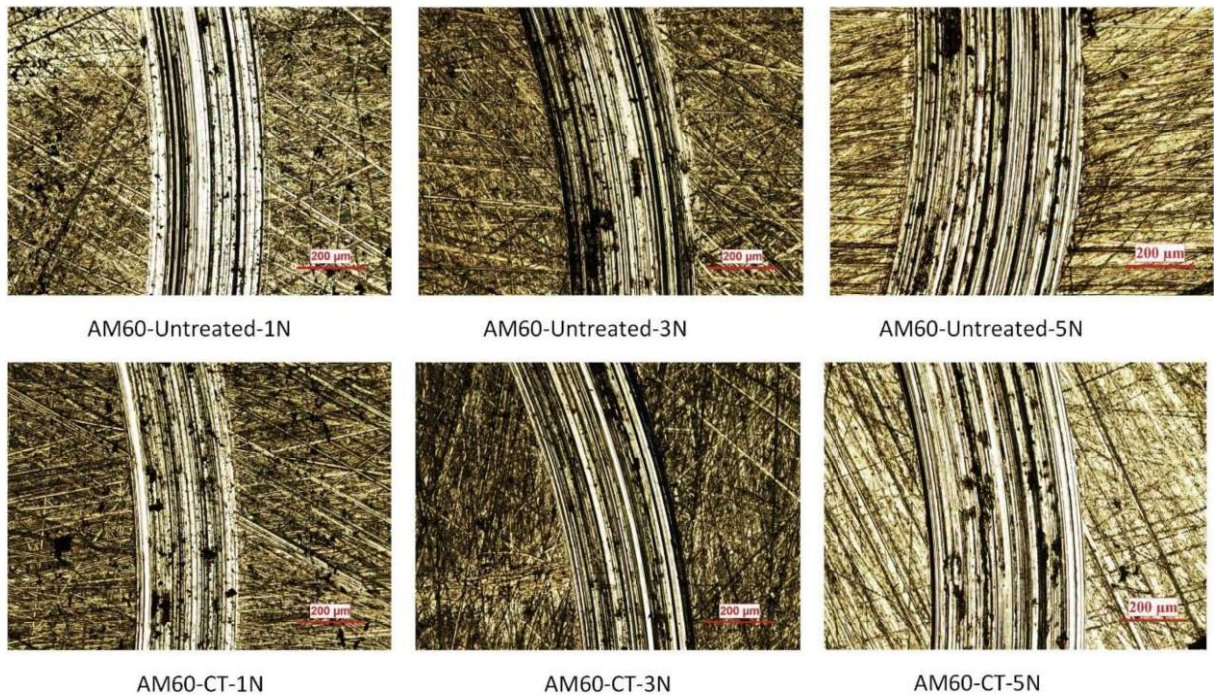


Figure 4.8. Worn surfaces of untreated and cryogenic treated AM60 wear tracks in a dry medium.

Figure 4.9 is a data representation of the values obtained from a microscopic imaging of the wear track of untreated and treated sample of AM60 Magnesium alloy, after undergoing an experiment where loads of 1 N, 3 N, and 5 N, were exerted on a rotating steel ball that came in contact with the surface of the sample. This was to assess the impact of the cryogenic treatment

on the wear performance of the samples under investigation in a wet medium. The 1 N load was exerted on the steel ball as the experiment was carried on and the result in terms of the wear track width for the untreated and treated samples in this wet medium were 385.9 μm and 464.7 μm respectively, with the untreated sample showing to have a 78.8 μm narrower wear track width. When the samples were exposed to the 3 N load, the untreated and treated samples showed wear track width values of 549.1 μm and 539.9 μm respectively, with the treated sample producing 9.2 μm narrower wear track width than the untreated sample. As the load was increased to 5 N, the values of their wear track width were seen to be 608 μm and 561 μm for the untreated and treated samples respectively, with the treated sample showing to have a 47 μm narrower wear track width. From the values that the samples being compared showed, we have learned that the untreated sample produces better wear resistance for the lowest load category, but the treated sample gradually and eventually showed better values in terms of wear resistance performance as the load was increased. That is an indicator that the cryogenic heat treatment is effective when the load is more on the samples. The ineffectiveness of the lower loads might be as a result of the chemical reactions that the medium in which the experiment is conducted (0.9 wt. % NaCl solution) has with the sample under investigations. As we can see that the level of corrosion wear is quite prominent on the samples. The wear on these samples tested in the wet medium is also seen to be more prolific than that of those conducted in the dry medium, this is mostly due to the chemical interaction between the sample and the wet medium, leading to corrosion wear.

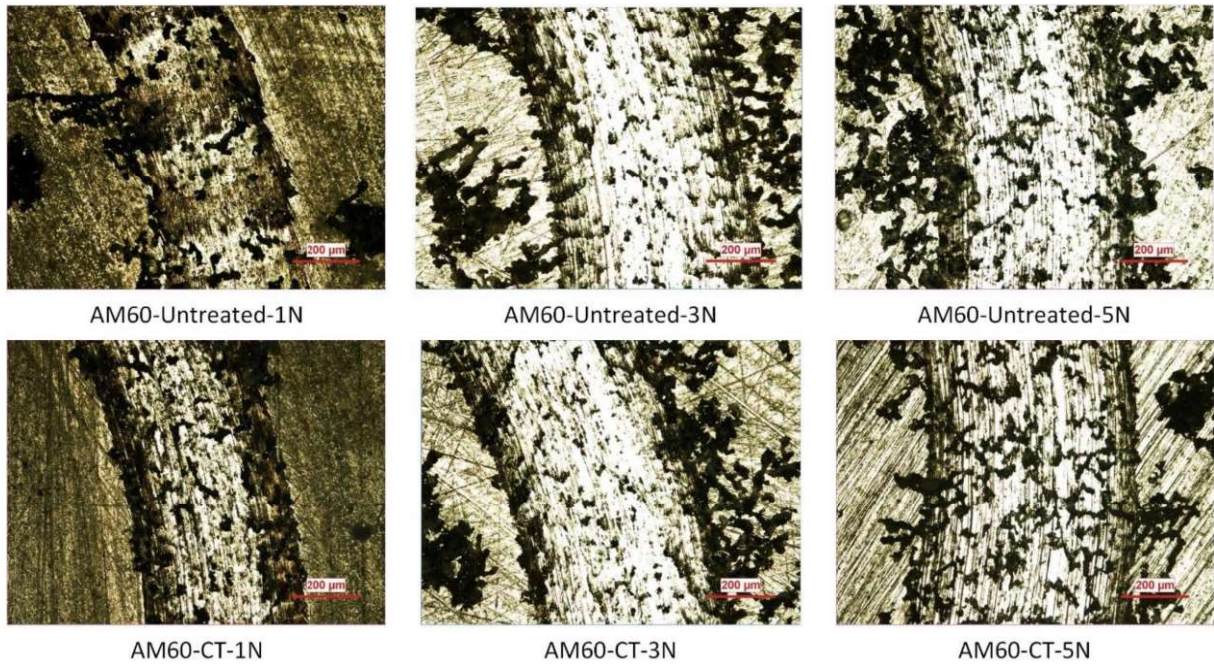


Figure 4.9. Worn surfaces of untreated and cryogenic treated AM60 wear tracks in a wet medium.

4.3.2. Specific wear rate and coefficient of friction behaviour

Figure 4 shows the wear tracks for the dry medium of the cross-sectional view of each specimen. The surface profile measurements were used to calculate the wear area and wear track width (dx) of the two samples (untreated AZ91Mg alloy and cryogenically treated AZ91). Regarding the base profile of the samples (peaks formation), abrasion, delamination, and plastic deformation mechanisms were predominant with a rough surface. When the samples were tested with the load of 1 N, the untreated sample showed a wear area of $1750 \mu\text{m}^2$ and a wear track width of 0.30 mm, whereas the treated sample showed a slightly larger wear area of $1830 \mu\text{m}^2$ and a wear track width of 0.31 mm (an area difference of $80 \mu\text{m}^2$). When the load of 3 N was exerted on the materials in the experiment, the untreated sample exhibited a wear area of $4440 \mu\text{m}^2$ and a wear track width of 0.45 mm. Alternatively, the treated sample showed a slightly larger wear area of $4480 \mu\text{m}^2$ and an identical wear track width of 0.45 mm (a wear area difference of $40 \mu\text{m}^2$).

When the load of 5 N was applied to the samples under the experiment, the untreated sample recorded a wear area of $7990 \mu\text{m}^2$, whereas the treated sample recorded a wear area of $7780 \mu\text{m}^2$ and a wear track width of 0.58 mm (a wear area difference of $210 \mu\text{m}^2$). According to the received data, the treated sample exhibited a better wear resistance with the addition of more load. The untreated sample showed a slightly better wear resistance when 1 N was applied, and that margin became smaller as the 3 N load was applied. Then, the treated sample became the material with a better wear resistance when the load applied was 5 N.

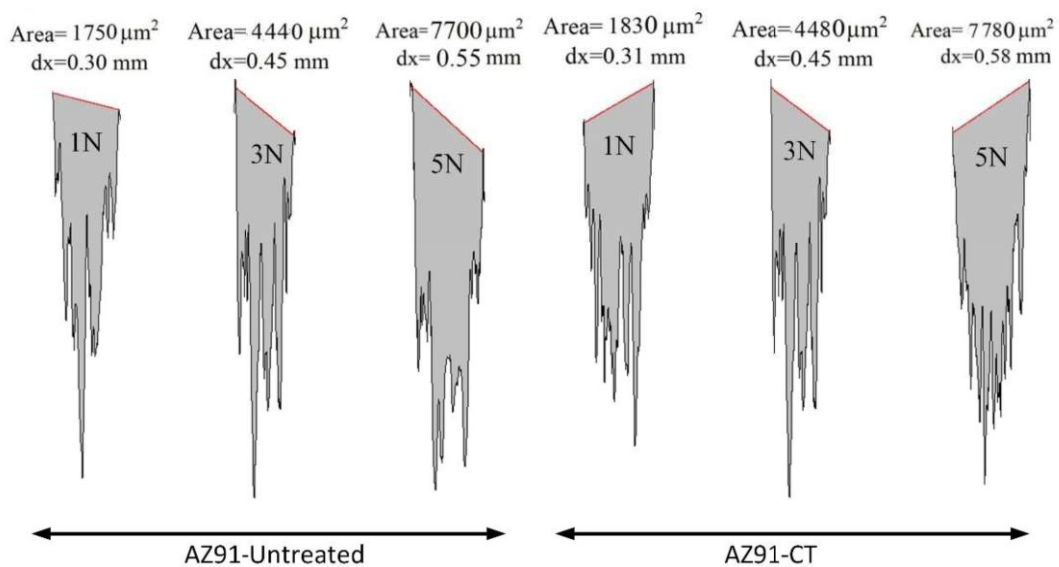


Figure 4.10. A cross-sectional view of untreated and cryogenic treated AZ91 wear track profiles in a dry medium.

Regarding the wet medium (Figure 5), when a load of 1 N was applied to both samples under the same conditions, the untreated sample was observed to register a wear area of $3406 \mu\text{m}^2$ and a wear track width of 0.46 mm. However, the treated sample registered a relatively lower wear area of $2734 \mu\text{m}^2$ and a wear track width of 0.41 mm, with an area difference of $672 \mu\text{m}^2$. When the load of 3 N was applied, the untreated sample registered a wear area of $4538 \mu\text{m}^2$ and a wear track width of 0.51 mm, whereas the treated sample under the same conditions and load registered a smaller wear area of $3643 \mu\text{m}^2$ and a wear track width of 0.51 mm, with an area difference of $895 \mu\text{m}^2$. When the load of 5 N was applied to the sample,

the untreated sample registered a wear area of $5006 \mu\text{m}^2$ and a wear track width of 0.55 mm , whereas the rival treated sample exhibited a wear area of $5472 \mu\text{m}^2$ and a wear track width of 0.53 mm , with a $434 \mu\text{m}^2$ area difference. The data also showed a bigger area margin with the middleweight applied, which recorded an area margin of $895 \mu\text{m}^2$, compared to the lowest load applied and the highest load applied, which registered area differences of $672 \mu\text{m}^2$ and $434 \mu\text{m}^2$ respectively. Comparing the cross-sectional images of the wear track of the wet medium to the dry medium, the profile of the wet medium had a very smooth profile.

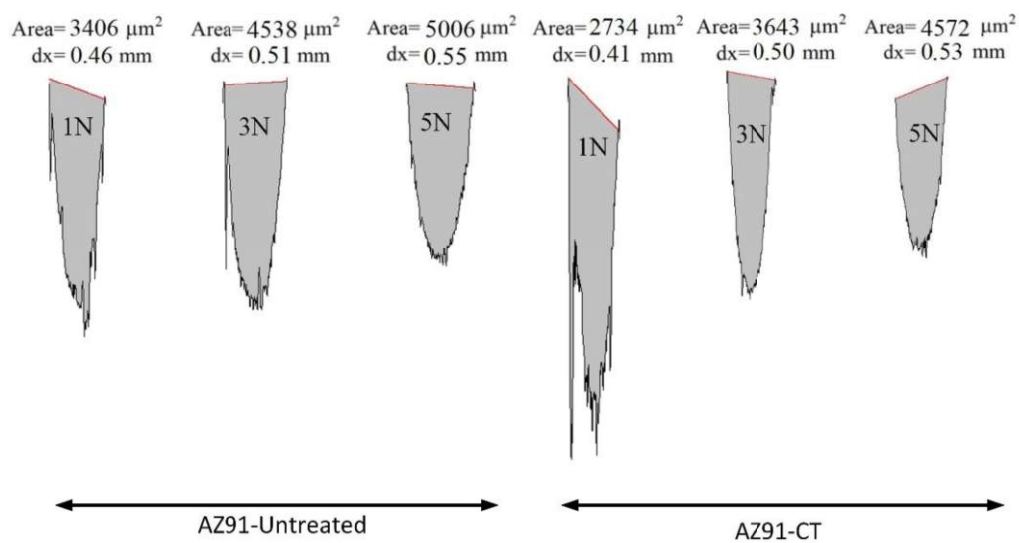


Figure 4.11. A cross-sectional view of untreated and cryogenic treated AZ91 wear track profiles in a wet medium.

Figure 4.12 is data collected from the investigation showing the wear area of the untreated and treated sample under loads of 1 N , 3 N , and 5 N in a dry medium. Comparing the wear areas of the two rival samples under the 1 N load, we see that the untreated sample has a wear area of $2230 \mu\text{m}^2$ and $dx=0.33 \text{ m}$ while the treated sample showed a wear area of $1700 \mu\text{m}^2$ and $dx = 0.30 \text{ m}$. The untreated sample showed $530 \mu\text{m}^2$ more worn area than the treated sample. At the 3 N load, the untreated sample was seen to record a wear area of $5960 \mu\text{m}^2$ and $dx = 0.54 \text{ m}$ while the treated sample had a wear area of $4560 \mu\text{m}^2$ and $dx = 0.45 \text{ m}$, the untreated sample having $1400 \mu\text{m}^2$ more wear area than the treated sample. When the load on the samples were adjusted to 5 N , the untreated sample showed are wear are of $8190 \mu\text{m}^2$ and $dx = 0.52 \text{ m}$

while the treated sample exhibited a wear area of $7850 \mu\text{m}^2$ and $dx = 0.55 \text{ m}$, a difference in wear area of $340 \mu\text{m}^2$ that the untreated sample has more than the treated sample. We have seen that the treated sample had a wide edge over the untreated sample in terms of wear resistance performance in the 1 N load category, at the 3 N load category an even wider disparity in terms of the wear resistance values were seen favoring the treated sample, but that slowed down with the 5 N load category, suggesting that the wear resistance increased from 1 N to 3 N but decreased from 3 N to 5 N.

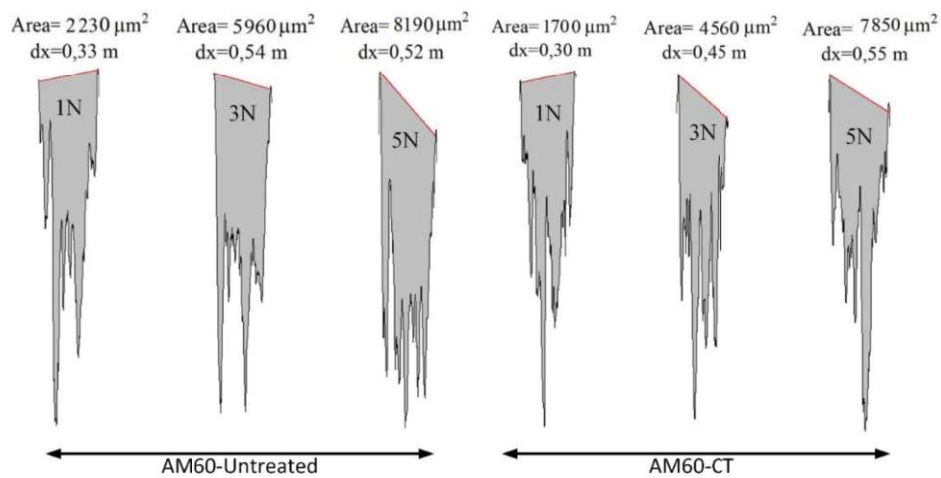


Figure 4.12. A cross-sectional view of untreated and cryogenic treated AM60 wear track profiles in a dry medium.

Figure 4.13 is a data representation of the values of wear areas of the untreated and treated sample of the AM60 alloys in a wet medium (0.9 wt. % NaCl solution being the medium in which the test was conducted) with the samples tested under 1 N, 3 N, and 5 N loads. When the 1 N load was exerted on the steel ball that took a rotational motion on the samples, a wear area of $2598 \mu\text{m}^2$ and $dx=0.42 \text{ m}$ was registered for the untreated sample while the treated sample registered a wear area of $3956 \mu\text{m}^2$ and $dx = 0.55 \text{ m}$, a difference in where area of $1358 \mu\text{m}^2$ that the treated sample has more than the untreated sample. When the 3 N load was exerted on both samples wear area values of $6200 \mu\text{m}^2$ $dx=0.56 \text{ m}$ and $6278 \text{ dx}=0.55$ were obtained for the untreated and treated samples respectively, a wear area difference of $78 \mu\text{m}^2$ that the treated sample has over the untreated sample. With the load adjusted to the 5 N load, the sample

provided wear area values of $5694 \mu\text{m}^2$ $dx = 57 \text{ m}$ and $6513 \mu\text{m}^2$ $dx = 67 \text{ m}$ for the untreated and treated samples respectively, a difference of $819 \mu\text{m}^2$ that the treated sample has over the untreated sample. It can be observed that the values of the wear area of the sample when loads from 1 N, 3 N, and 5 N were placed on the samples under test in the wet medium, the untreated sample is seen to show a better wear resistance performance base on the wear area of the sample, with the lowest load showing the largest wear area difference, the middle load showing almost the same values while the highest load showing the second largest value of wear area difference. This is despite the situation that the opposite happened in the dry medium, where the treated sample showed better wear resistance in terms of wear area and that the middle load showed a larger difference in the wear area. From these two results, we could suggest that the fluctuation in the wear performances of the sample was base on the effect of the wet medium on the samples.

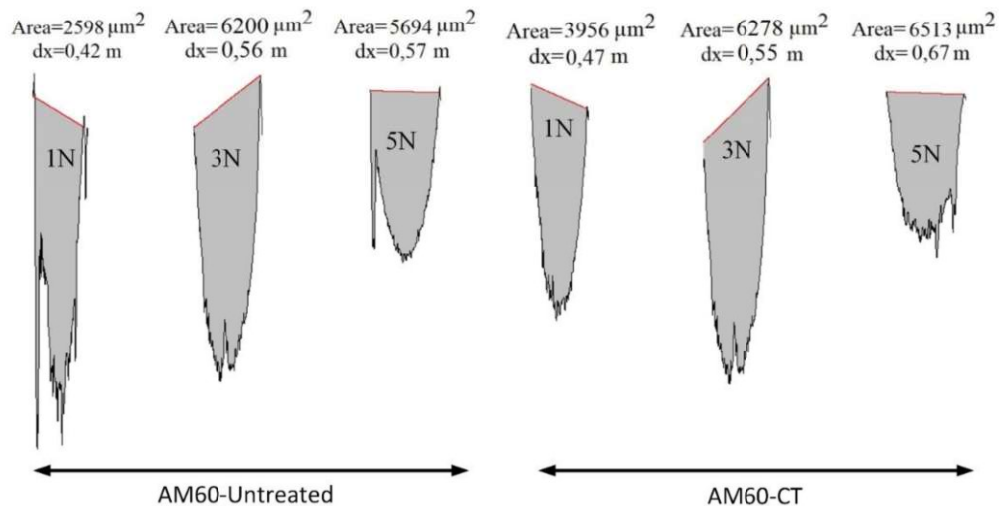


Figure 4.13. A cross-sectional view of untreated and cryogenic treated AZ91 wear track profiles in a wet medium.

Figure 4.14 represents the values of the SWR or the wear resistance of the specimens corresponding to the different loads that were applied to the samples during the experiment for the dry medium. This value, the SWR (W_s) was extracted from Eq. (4.1). In this formula, the volume loss, applied load, and sliding distance were presented as ΔV , L , and d , respectively.

The volume loss in the equation was found by multiplying the cross-sectional area of the wear tracks by the length of the wear tracks.

$$W_s = \frac{\Delta V}{L.D} \left[\frac{mm^3}{N.m} \right] \quad (4.1)$$

The findings on the graph show that, when the load of 1 N was applied to both samples under the same conditions, the untreated sample has a relatively lower SWR. As the load increased to 3 N, the SWRs between the two samples were almost the same as the untreated sample, showing a slightly lower SWR. The plots show almost the same values as the load was further increased to 5 N, again with the untreated sample having a slightly lower SWR. This indicates that the wear rates for the dry medium are more favorable in the untreated sample when a lower load is applied but gradually shifts to favor the treated sample as the load increases.

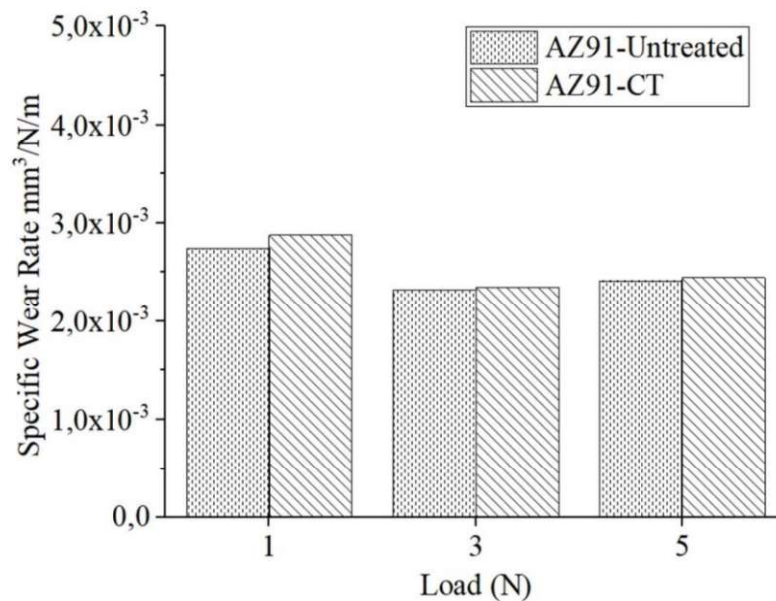


Figure 4.14. The specific wear rate of untreated and cryogenic treated AZ91 in a dry medium.

Regarding the wear resistance of the treated AZ91 in the wet medium, the initial load of 1 N shows a relatively large margin between the untreated sample compared to the treated sample, with the treated sample showing a relatively lower SWR by a large margin (Figure 4.15). At the 3 N load, the treated sample still shows a relatively lower SWR when compared to

the rival untreated sample, but the margin decreased with the addition of the load. At the 5 N load, the difference in the SWR was very little despite the treated sample still having a relatively lower SWR of the two samples. The treated sample showed better performance compared to the untreated sample for all loads applied in the wet medium.

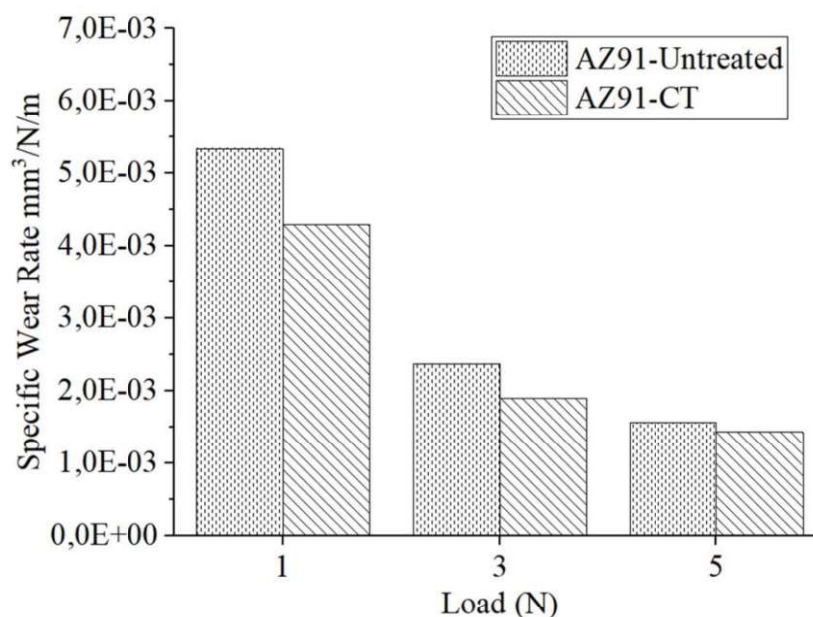


Figure 4.15. The specific wear rate of untreated and cryogenic treated AZ91 in a wet medium.

Figure 4.16 shows wear rate values of cryogenically treated and untreated samples of AM60 alloy that underwent some wear test under load classes of 1 N, 3 N, and 5 N in a dry pin-on-disc test. The wear rate of a material is the volume of the material lost per unit distance. The experimental condition such as; distances covered, interacting material and its speed while interactions were the same and constant for all the samples involved. The data comparison between the untreated and treated sample in the 1 N load category revealed that the wear rates comparison between the untreated and the treated sample in the experiment have a difference of approximately $0.8 \times 10^{-3} \text{ mm}^3/\text{N/m}$, with the untreated sample seen to have the higher wear rate of the two samples being compared. As the load was shifted to the 3 N category, the untreated sample was again seen to have a higher wear rate by approximately $0.7 \times 10^{-3} \text{ mm}^3/\text{N/m}$ when compared to the treated sample in the experiment. When the load of 5 N was exerted on the samples, the difference was at this time seem to approximately $-0.15 \times 10^{-3} \text{ mm}^3/\text{N/m}$, still in

favor of the treated sample in the context of better wear resistance performance but with a much smaller difference compared to the previous weight categories. We have seen from this investigation that the treated sample has had a much bigger edge over the untreated sample when the load exerted on the samples was the smallest, then that difference is seen to shrink as the load was increased to the middle load used in this experiment and finally got even smaller with the largest load used in the experiment. It is seen that the effectiveness of the cryogenic treatment of the samples were more conspicuous in the lower loads of the experiment. A similar result was seen from the wear track width and the wear area absorbed. The general result also confirmed that the wear rate of the samples is independent of load used on the sample

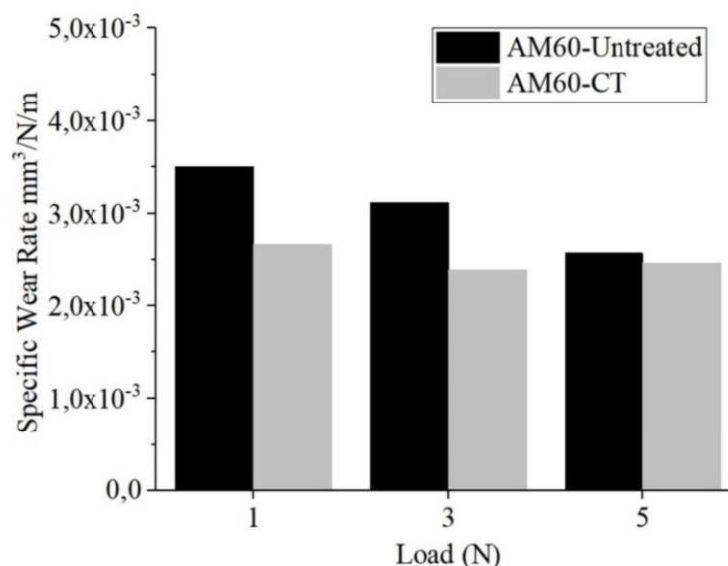


Figure 4.16. The specific wear rate of untreated and cryogenic treated AM60 in a dry medium.

Figure 4.17 is the data representation of values that were collected from the wear experiment seeking to find the wear rates of the samples in a wet pin-on-disc test of treated and untreated AM60 alloys. With all other experimental conditions the same and constant, loads of 1 N, 3 N, and 5 N were used to find the difference between the untreated and untreated samples in terms of their wear rates. the solution used as the host to simulate a wet medium was 0.9 wt.% NaCl solution. The experimental values shown when the 1 N load was applied on the steel ball showed that the untreated sample had a wear rate that was approximately $2.1 \times 10^{-3} \text{ mm}^3/\text{N/m}$

less than the wear rate values shown by the treated sample in the wet medium. As the load was added to 3 N, the two samples were seen to have almost the same wear rate values with the untreated sample showing a slight edge of approximately $0.5 \times 10^{-3} \text{ mm}^3/\text{N}/\text{m}$ over the treated sample in terms of less wear rate. When the load was added to 5 N, the results showed that the untreated sample at this time has an approximately $2 \times 10^{-3} \text{ mm}^3/\text{N}/\text{m}$ less than the value produced by the treated sample in the wet medium. The value shown in this experiment is opposite to those produced in the dry medium. These values shown that at the lowest load applied, the cryogenic treatment seems to promote the wear of the material under investigation as the values produced in terms of their difference in wear rate were so far apart with the untreated sample being the one to look for as far as good wear resistance is concern in that weight category. The middle and largest loads used in the experiment did not show a high contrast in the wear rate of the samples but they still show that the untreated sample was still somehow better in terms of wear resistance in the wet environment that we simulated. Similar results were seen form the above analysis in the wear track width and the wear area. This tells us that the cryogenic treated was not effective for the weight categories that we have tested.

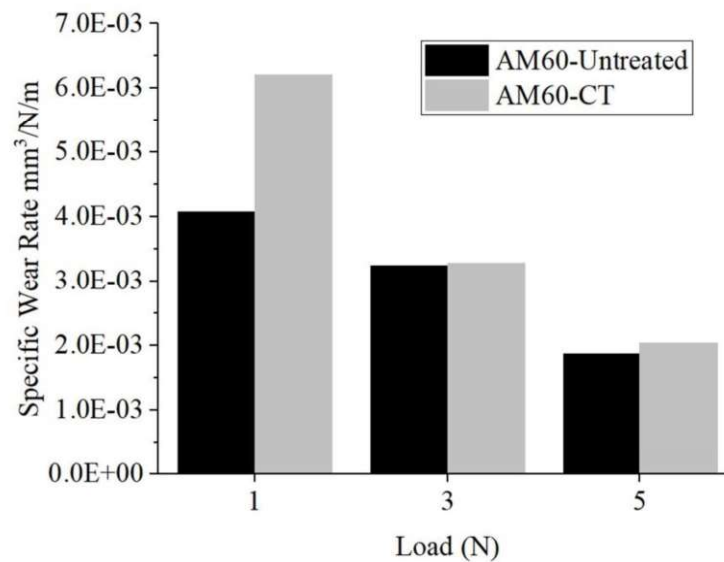


Figure 4.17. The specific wear rate of untreated and cryogenic treated AM60 in a wet medium.

The COF is normally not considered to be connected to the wear rate of the material. Figure 4.18 is an illustration of the value of the COF of the untreated and treated AZ91 magnesium alloys in the dry medium under loads of 1 N, 3 N, and 5 N. The values have shown that, for all the load categories (with the exception of the 3 N) for both untreated and treated samples, the COF of each material had the most significant increase in the first 0.75 m of the total 10 m for the remaining 9.25 m of the load categories in question, and the COF remained almost constant. The values for the 3 N load category for both untreated and treated materials were almost constant from the beginning of the test to the end of the 10 m. From the overall values, the untreated AZ91 showed a greater COF value than all the other samples in the dry medium. To a large extent, this is a result of the higher load value of the sample in question relative to the other samples in the experiment, except for the treated AZ91, which also bears the same load as the sample in question. The explanation that could be used to justify the disparity in the values of the two samples despite bearing the same load is that one is cryogenically treated and the other is not. Therefore, cryogenic treatment affects the values of their COF, which determines the level of wear that the materials will endure to some degree. The untreated sample with the 1 N load had the lowest COF, while the treated sample bearing the same load has a relatively higher COF value. As shown in the previous results, this means that the CT is not effective in the wear resistance in instances in which the applied weight is low. The untreated and treated samples under the 3 N load showed COF values that are not far apart, with the untreated sample again showing slightly better COF values.

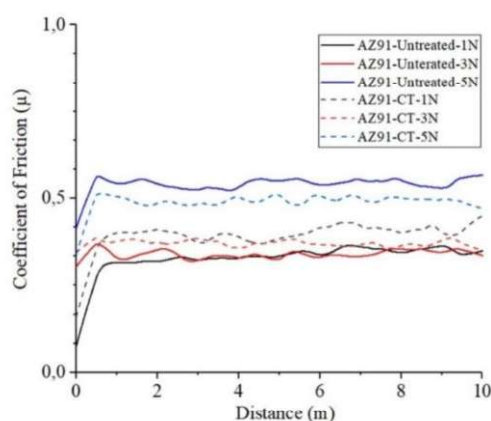


Figure 4.18. Coefficient of friction of untreated and cryogenic treated AZ91 in a dry medium.

The values of the COF obtained from the wet medium are significantly less than those from the dry medium, which is primarily due to the presence of some lubrication in the wet medium (Figure 4.19). In this experiment, almost all the values are not far apart from each other. The treated and untreated samples for the load of 1 N and the treated sample at the 3 N load, which are all at different distances within the 10 m distance of the test, have the lowest COF, which fluctuated among them. For the first 5 m, the treated sample under the 5 N load had a higher COF than all the other samples in the experiment in the wet medium, but it showed lower COF values than the untreated sample after the 5-m mark. This suggests that the CT is still effective in the wet medium.

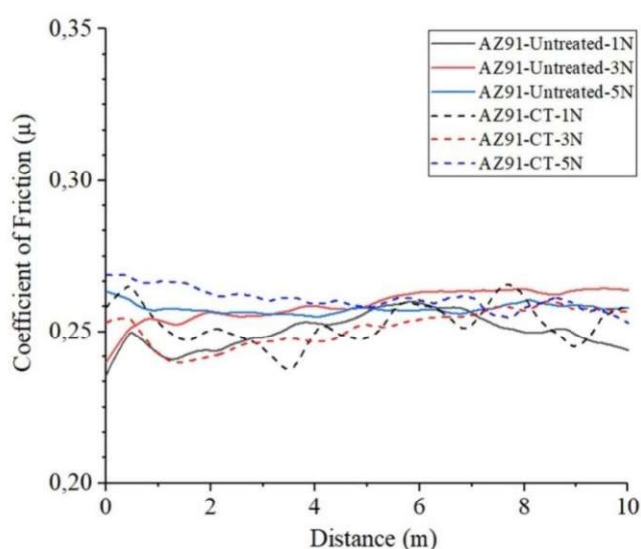


Figure 4.19. Coefficient of friction of untreated and cryogenic treated AZ91 in a wet medium.

Figure 4.20 is the data collected from the test showing the coefficient of friction between the steel ball and the untreated and cryogenically treated samples in the dry medium. the test was conducted with the samples exposed to a load range of 1 N, 3 N and 5N. For the results shown by the samples the bear the 1 N load, we see a relatively big difference in the values of COF that the two samples showed. The untreated sample is seen to have an almost steady value from the beginning of the test towards the 10 m distance that the test was conducted and showed values around 0.25 μ while the treated sample started the test around COF value of 0.33 μ but those value quickly rose to 0.58 μ within the first 0.5 m of the test and remained somewhat

constant in that value for the rest of the 10 m of the test. When a 3 N load was put on the samples during the test it was seen that the untreated sample started the test with a COF value of around 0.33μ and remained somewhat constant for the rest of the 10 m test under the same weight class. However, the treated sample started at a slightly lower value of COF which was around 0.26μ but the value quickly increased to around 0.46μ where the value would remain somewhat constant until around the 8 m in the test where they drop to 0.41μ for the rest of the 10 m distance. The 5 N load category showed the values of COF of the samples to not have shown any major difference. In this case, the untreated sample started a much lower COF value than the treated sample but within 0.5 m in the experiment, both samples went back and with almost the same COF values towards the end of the 10 m test when both are seen to have the same value at the 10 m distance. In the overall results, we have seen that the untreated sample under the 5 N load had the lowest COF value for the whole test and the treated sample under the 5 N load had the highest COF value for the whole test.

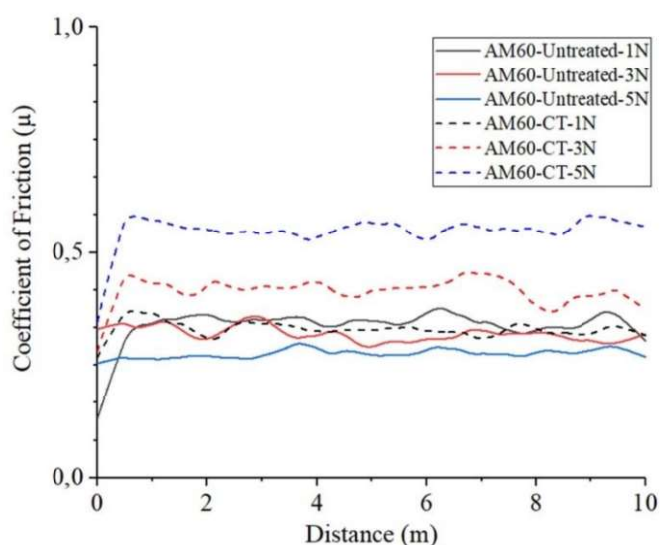


Figure 4.20. Coefficient of friction of untreated and cryogenic treated AM60 in a dry medium.

Figure 4.21 is a graph that displays the results of data that was collecting from the pin-on-disc wear that was conducted in a wet medium (0.9 wt.% NaCl solution). A cryogenically treated and untreated sample that were exposed to loads of 1 N, 3 N and 5 N were the subjects of the invention where there COF of frictions were to be assed. At the 1 N load, the untreated

sample was seen to have started the experiment with the second-highest COF values but the value dropped around the 0.5 m of the 10 m; to the be within the samples the exhibit the lower value, then 4 m in the test it even dropped futher to separate itself as the sample with the lowest COF value. However, the treated sample was seen to record COF value of around 0.31 μ ; a value that stands out as the hight COF recorded amongst all the samples within the test, to start the test. The value dropped around 4 minutes in the test to the level of the other samples in the test but eventually went up again to end the test as the sample with the highest COF value recorded. All the other samples in the test recorded COF values that were not far apart from each other except for the sample that had the 1 N load on them. The COF values in this wet medium could be seen to be much lower than the values that were seen with the samples in the dry medium, this major difference could be attributed to the lubricating effects that the medium in which the test was conducted had on the interaction between the sample and the steel ball. This could be the same reason for the less wear experienced by the sample in the wet medium compared to the samples in the dry medium. The behavior is shown by the sample at the 1 N load (both treated and untreated) at the wet medium as seen to be the same behavior shown by samples bearing the 5 N load in the dry medium. this again goes to qualify the knowing that the COF cannot be used to qualify the level of wear that a sample endures as shown by various researchers.

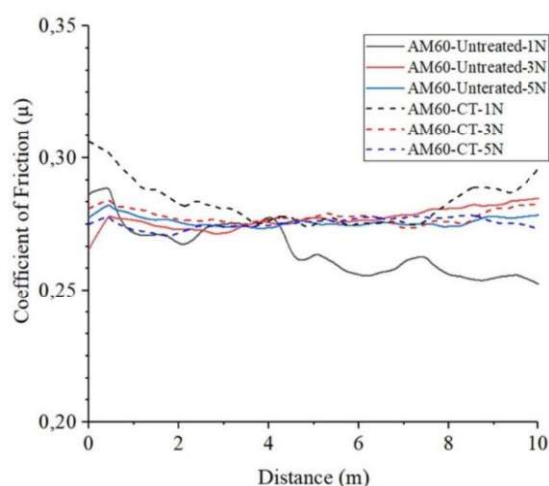


Figure 4.21. Coefficient of friction of untreated and cryogenic treated AM60 in a wet medium

5. CONCLUSIONS AND RECOMMENDATIONS

In this study, the corrosion behavior of cryogenic treated AZ91 and AM60 alloy compared to that of the non-cryogenic treated AZ91 and AM60 in the 0.9 wt.% NaCl solution was evaluated. On the other hand, the comparison of the wear behaviors between untreated AZ91 alloys and a treated AZ91 alloy in both a dry and wet media with the wet medium being a 0.9 wt.% NaCl solution. In general, the cryogenically treated alloy showed better corrosion resistance and wear resistance, the following conclusion can be drawn:

Corrosion results;

- The cryogenic treatment changed the microstructure of AZ91 and AM60; formation of new twin phases like needle and drastically diminish the eutectic phases were observed.
- Overall, the corrosion resistance in 0.9 wt.% NaCl solution was relative higher for the cryogenic treated AZ91 and AM60 sample compared to the untreated sample.
- For AZ91, E_{pit} values of -1.25 mV and -1.40 V where observed for the treated and untreated samples, respectively, further showing that pitting corrosion was more going more rapidly with the untreated sample. A steeper slope on the passivation zone of the treated sample was also observed, showing that the efforts to slow down the ongoing corrosion was stronger on the side of the treated sample.
- For AM60, E_{pit} values of -1.15 V and -1.07 V where seen for the treated and untreated samples, respectively, reaffirming the dominance of pitting corrosion on the untreated sample more than in is on the treated sample (even though the difference is not that significant). A slightly longer slope of passivation slope showed by the treated sample was also seen, telling us that the treated sample has a lightly more resilience toward the corrosion activity toward it.
- Impedance analysis showed a slightly more favorable corrosion resistance behavior of treated alloy with a higher loop when compared to the rival sample.

Wear results;

- For dry sliding, for the larger the load, the cryogenic treatment was more effective on the treated sample. For wet sliding, the cryogenic treatment was more effective on the lesser loads in terms of the wear track width and wear area.
- For the dry medium, the untreated sample has a slight (almost insignificant) SWR. However, the treated sample has a better SWR than the opponent sample in the wet medium, but the difference in the SWR reduces with the increase in the load.
- The untreated sample has a lower COF at lower loads, but that changes with the increase in the load in the dry medium. The COF is within a similar range for all the samples, suggesting that it cannot be used as a parameter to determine which samples are superior in terms of wear performance because many other factors could affect the values of the COF in a wet medium.
- The samples in the wet medium are relatively lower in wear areas and have lower COF values, which could be attributed to the lubricating effects of the solution.
- For AM60; the wear track width showed results that indicate the effectiveness of the cryogenic treatment of the sample when in a dry medium. the treated sample showed narrower wear track width when compared to the untreated sample, and the more load exerted on the steel ball, the values get even better for the wear resistance compared to the rival sample.
- However, the results in the wet medium were different in the wet medium, with the untreated sample showing better values as far as wear track width in the lowest load, but when the 3 N load used the values were almost the same for both samples and the 5 N load show the effectiveness of the cryogenic treatment by show better wear track values for the treated sample.

- The wear cryogenic heat treatment enhanced the wear performance of the treated sample AM60 at the lower weight to the medium weight, even producing a better wear resistance performance from the lowest weight to the medium weight but the wear resistance performance began to take some drawback at the highest weight used in the test for the test in the dry medium, meaning that the cryogenic treatment was effective in enhancing the wear behavior of the AM60 magnesium alloy in a dry medium.
- However, the wet medium provides a different result from the samples. The untreated sample AM60 was seen to be more wear resistance based on the wear area; this is mainly due to the fact that the sample has with the solution in which they are being tested.
- For the results of the wear rate of AM60, the effectiveness of the cryogenic treatment of the sample was more clear at the lower loads, as it is seen that the rate decreased with the addition of weight. This is consistent with the results seen from the wear track width. However, the wet medium showed that the cryogenic treatment was not effective in the enhancement of the wear performance with the loads that were used in the test.

REFERENCES

- Aatthisugan, I., Razal Rose, A., Selwyn Jebadurai, D., 2017, Mechanical and wear behaviour of AZ91D magnesium matrix hybrid composite reinforced with boron carbide and graphite. *J. Magnes. Alloy*, 5(1): 20-25, doi:<https://doi.org/10.1016/j.jma.2016.12.004>.
- Abbott, T., Cáceres, C., Easton, M., 2004, *Design with Magnesium: Alloys, properties and casting processes*. pp. 487-538.
- Abdelaziz, M.H., Paradis, M., Samuel, A.M., Doty, H.W., Samuel, F.H., 2017, Effect of Aluminum Addition on the Microstructure, Tensile Properties, and Fractography of Cast Mg-Based Alloys. *Advances in Materials Science and Engineering*, 2017: 7408641, doi:10.1155/2017/7408641.
- Akyüz, B., 2019, Wear and machinability of AM series magnesium alloys. *Mater. Test*, 61(1): 49-55, doi:10.3139/120.111285.
- Amini, K., Akhbarizadeh, A., Javadpour, S., 2014, Investigating the effect of quench environment and deep cryogenic treatment on the wear behavior of AZ91. *Materials & Design (1980-2015)*, 54: 154-160, doi:<https://doi.org/10.1016/j.matdes.2013.07.051>.
- Asl, K.M., Tari, A., Khomamizadeh, F., 2009a, Effect of deep cryogenic treatment on microstructure, creep and wear behaviors of AZ91 magnesium alloy. *Materials Science and Engineering: A*, 523(1–2): 27-31, doi:<http://dx.doi.org/10.1016/j.msea.2009.06.003>.
- Asl, K.M., Tari, A., Khomamizadeh, F., 2009b, Effect of deep cryogenic treatment on microstructure, creep and wear behaviors of AZ91 magnesium alloy. *Mater. Sci. Eng., A*, 523(1): 27-31, doi:<https://doi.org/10.1016/j.msea.2009.06.003>.

REFERENCES (continue)

- Avedesian, M.M., Baker, H., 1999, ASM Specialty Handbook: Magnesium and Magnesium Alloys, Avedesian, M.M., Baker, H., Eds., ASM International: USA,
- Bhavar, V., Khot, S., Kattire, P., Mehata, M., Singh, R., 2015, Effect of Deep Cryogenic Treatment on AISI H-13 Tool Steel. October 20-22; pp. 383-389.
- Bommala, V.K., Krishna, M.G., Rao, C.T., 2019, Magnesium matrix composites for biomedical applications: A review. J. Magnes. Alloy, 7(1): 72-79, doi:<https://doi.org/10.1016/j.jma.2018.11.001>.
- Botelho, P.A.D.O., 2015, Biodegradable stents made of pure Mg and AZ91 alloy through SPS sintering. University of Trento, 80.
- C. Moosbrugger, E., 2017, Engineering Properties of Magnesium Alloys, ASM International: Ohio, USA,
- Callister, W.D., Rethwisch, D.G., 2020, Callister's Materials Science and Engineering, Wiley:
- Cardarelli, F., 2013, Materials Handbook: A Concise Desktop Reference, Springer London:
- Chelliah, N.M., Kumar, R., Singh, H., Surappa, M.K., 2017, Microstructural evolution of die-cast and homogenized AZ91 Mg-alloys during dry sliding condition. J. Magnes. Alloy, 5(1): 35-40, doi:<https://doi.org/10.1016/j.jma.2017.02.001>.
- Chelliah, N.M., Padaikathan, P., Kumar, R., 2019, Evaluation of electrochemical impedance and biocorrosion characteristics of as-cast and T4 heat treated AZ91 Mg-alloys in Ringer's solution. J. Magnes. Alloy, 7(1): 134-143, doi:<https://doi.org/10.1016/j.jma.2019.01.005>.

REFERENCES (continue)

- Chelliah, N.M., Singh, H., Surappa, M.K., 2016, Correlation between microstructure and wear behavior of AZX915 Mg-alloy reinforced with 12 wt% TiC particles by stir-casting process. *J. Magnes. Alloy*, 4(4): 306-313, doi:<https://doi.org/10.1016/j.jma.2016.09.002>.
- Demir, A.G., Previtali, B., Ge, Q., Vedani, M., Wu, W., Migliavacca, F., Petrini, L., Biffi, C.A., Bestetti, M., 2014, Biodegradable magnesium coronary stents: material, design and fabrication. *Int. J. Comput. Integ. M.*, 27(10): 936-945, doi:10.1080/0951192X.2013.834475.
- Dieringa, H., Kainer, K.U., 2007, Magnesium – der Zukunftswerkstoff für die Automobilindustrie? , *Materialwissenschaft und Werkstofftechnik*, 38(2): 91-96, doi:10.1002/mawe.200600114.
- Ding, W., 2016, Opportunities and challenges for the biodegradable magnesium alloys as next-generation biomaterials. *Regen. Biomater.*, 3(2): 79-86, doi:10.1093/rb/rbw003.
- Dunmade, I., 2012, Effect of Rolling on the Formability of Aluminum Alloy 5454 Series as a Potential Material Substitute for Agri-Industrial Applications. *International Journal of Materials Science*, 7: 203.
- Dziubińska, A., Surdacki, P., Dziubiński, M., Barszcz, M., 2016, The forming of magnesium alloy forgings for Aircraft and Automotive applications. *Advances in Science and Technology Research Journal*, 10: 158-168, doi:10.12913/22998624/64003.

REFERENCES (continue)

- Esmaily, M., Svensson, J.E., Fajardo, S., Birbilis, N., Frankel, G.S., Virtanen, S., Arrabal, R., Thomas, S., Johansson, L.G., 2017, Fundamentals and advances in magnesium alloy corrosion. *Prog. Mater. Sci.*, 89: 92-193, doi:<https://doi.org/10.1016/j.pmatsci.2017.04.011>.
- Friedrich, H.E., Mordike, B.L., 2006, *Magnesium Technology: Metallurgy, Design Data, Applications*, Springer Berlin Heidelberg:
- García-Rodríguez, S., Torres, B., Maroto, A., López, A.J., Otero, E., Rams, J., 2017, Dry sliding wear behavior of globular AZ91 magnesium alloy and AZ91/SiCp composites. *Wear*, 390-391: 1-10, doi:<https://doi.org/10.1016/j.wear.2017.06.010>.
- Gassama, B., Öteyaka, M.Ö., 2019, Influence of cryogenic treatment on the corrosion of AZ91 and AM60 magnesium alloys in an isotonic solution. *Mater. Test*, 61(11): 1039-1044, doi:10.3139/120.111420.
- Gloria, A., Montanari, R., Richetta, M., Varone, A., 2019, Alloys for Aeronautic Applications: State of the Art and Perspectives. *Metals*, 9(6): 662.
- H., D., 2017, Influence of Cryogenic Temperatures on the Microstructure and Mechanical Properties of Magnesium Alloys: A Review., *Metals*, 7(2): 38.
- Hoche, H., Allebrandt, D., Scheerer, H., Broszeit, E., Berger, C., 2007, Design of wear and corrosion resistant PVD-coatings for magnesium alloys. *Materialwissenschaft und Werkstofftechnik*, 38(5): 365-371, doi:10.1002/mawe.200700143.
- Hu, T., Yang, C., Lin, S., Yu, Q., Wang, G., 2018, Biodegradable stents for coronary artery disease treatment: Recent advances and future perspectives. *Mater Sci Eng C Mater Biol Appl*, 91: 163-178, doi:10.1016/j.msec.2018.04.100.

REFERENCES (continue)

- Ilanaganar, E., Anbuselvan, S., 2018, Wear mechanisms of AZ31B magnesium alloy during dry sliding condition. *Mater. Today-Proc.*, 5(1, Part 1): 628-635, doi:<https://doi.org/10.1016/j.matpr.2017.11.126>.
- Jia, P., Wu, M., Zhang, J., Hu, X., Teng, X., Zhao, D., Wei, T., Dong, D., Liu, Q., Wang, Y., 2018, Effects of Mg–Zn–Y quasicrystal addition on the microstructures, mechanical performances and corrosion behaviors of as-cast AM60 magnesium alloy. *Materials Research Express*, 5: 106512, doi:10.1088/2053-1591/aada70.
- Jiang, Y., Chen, D., Chen, Z., Liu, J., 2010a, Effect of Cryogenic Treatment on the Microstructure and Mechanical Properties of AZ31 Magnesium Alloy. *Mater. Manuf. Process*, 25(8): 837-841, doi:10.1080/10426910903496862.
- Jiang, Y., Ding, C., Chen, Z., Liu, J., 2010b, Effect of Cryogenic Treatment on the Microstructure and Mechanical Properties of AZ31 Magnesium Alloy, Vol. 25, pp. 837-841.
- Klassen, R.D., Roberge, P., Lafront, A.M., Öteyaka, M., Ghali, E., 2005, Corrosion behaviour of zinc and aluminum magnesium alloys by scanning reference electrode technique (SRET) and electrochemical noise (EN). *Can. Metall. Q.*, 44: 47-52, doi:10.1179/000844305794409643.
- Klassen, R.D., Roberge, P.R., Lafront, A.M., Öteyaka, M.Ö., Ghali, E., 2003, Magnesium: Proceedings of the 6th International Conference Magnesium Alloys and Their Applications. April 28 - 30; pp. 655-660.
- Kramer, D.A., 2001, *Magnesium, its alloys and compounds*; p 29

REFERENCES (continue)

- Kumar, A., Kumar, S., Mukhopadhyay, N.K., 2018, Introduction to magnesium alloy processing technology and development of low-cost stir casting process for magnesium alloy and its composites. *J. Magnes. Alloy*, 6(3): 245-254, doi:<https://doi.org/10.1016/j.jma.2018.05.006>.
- Kumar, D., Jain, J., Bisht, T., Zindal, A., 2015, Effect of Precipitates on Mechanical and Tribological Performance of AZ91 Magnesium Alloy–Steel Couple. *137(2)*: 021604, doi:10.1115/1.4029248.
- Li, G.-r., Wang, H.-m., Cai, Y., Zhao, Y.-t., Wang, J.-j., Gill, S.P.A., 2013, Microstructure and mechanical properties of AZ91 magnesium alloy subject to deep cryogenic treatments. *International Journal of Minerals, Metallurgy and Materials*, 20(9): 896-901, doi:10.1007/s12613-013-0812-6.
- Li, J., Jiang, X.Q., 2011, Effect of Cryogenic Treatment on the Microstructure and Mechanical Properties of AZ31 Magnesium Alloy. *Materials Science Forum*, 686: 53-56, doi:10.4028/www.scientific.net/MSF.686.53.
- Liu, J., Li, G., Chen, D., Chen, Z., 2012, Effect of Cryogenic Treatment on Deformation Behavior of As-cast AZ91 Mg Alloy. *Chinese J. Aeronaut.*, 25(6): 931-936, doi:[https://doi.org/10.1016/S1000-9361\(11\)60464-0](https://doi.org/10.1016/S1000-9361(11)60464-0).
- Maldar, A., Ebrahmi, R., Davoodi, A., 2010, The Effect of Homogenization on Microstructure and Hot Ductility Behaviour of AZ91 Magnesium Alloy. *Kovove Mater.*, 48: 277-287, doi:10.4149/km_2010_5_277.
- Mao, L., shen, L., Chen, J., Zhang, X., Kwak, M., Wu, Y., Fan, R., Zhang, L., Pei, J., Yuan, G., et al., 2017, A promising biodegradable magnesium alloy suitable for clinical vascular stent application. *Sci. Rep-UK*, 7: 46343, doi:10.1038/srep46343.

REFERENCES (continue)

- Mert, F., 2017, Wear behaviour of hot rolled AZ31B magnesium alloy as candidate for biodegradable implant material. *T. Nonferr. Metal. Soc.*, 27(12): 2598-2606, doi:[https://doi.org/10.1016/S1003-6326\(17\)60287-5](https://doi.org/10.1016/S1003-6326(17)60287-5).
- Meshinchi Asl, K., Masoudi, A., Khomamizadeh, F., 2010, The effect of different rare earth elements content on microstructure, mechanical and wear behavior of Mg–Al–Zn alloy. *Mater. Sci. Eng., A*, 527(7): 2027-2035, doi:<https://doi.org/10.1016/j.msea.2009.11.061>.
- Mohan Lal, D., Renganarayanan, S., Kalanidhi, A., 2001, Cryogenic treatment to augment wear resistance of tool and die steels. *Cryogenics*, 41(3): 149-155, doi:[https://doi.org/10.1016/S0011-2275\(01\)00065-0](https://doi.org/10.1016/S0011-2275(01)00065-0).
- Oteyaka, M., Ghali, E., Tremblay, R., 2012a, Corrosion Behaviour of AZ and ZA Magnesium Alloys in Alkaline Chloride Media. *Int. J. Corr.*, 2012: 1-10, doi:10.1155/2012/452631.
- Oteyaka, M.O., Ghali, E., Tremblay, R., 2012b, Corrosion Behaviour of AZ and ZA Magnesium Alloys in Alkaline Chloride Media. *Int. J. Corr.*, 2012: 10, doi:10.1155/2012/452631.
- Öteyaka, M.Ö., 2002, Influence de L'addition de Ca Et Sr Sur la Corrosion Dans Des Solutions Aqueuses Des Alliages de Magnesium AZ Et ZA. Laval University, 172.
- Öteyaka, M.Ö., Lafort, A.M., Ghali, E., Tremblay, R., 2003, Potentiodynamic Studies of Some AZ and ZA Magnesium Alloys in Different Corrosive Media. In *Proceedings of Magnesium: Proceedings of the 6th International Conference Magnesium Alloys and Their Applications*, April 28 - 30; pp. 517-523.

REFERENCES (continue)

- Preciado, M., Bravo, P.M., Alegre, J.M., 2006, Effect of low temperature tempering prior cryogenic treatment on carburized steels. *Journal of Materials Processing Technology*, 176(1): 41-44, doi:<https://doi.org/10.1016/j.jmatprotec.2006.01.011>.
- Sato, A., Seiji, M., 1973, Electron microscopic observations of leukoplakia. *Archiv für dermatologische Forschung*, 247(3): 211-220, doi:10.1007/BF00596240.
- Shengfa, L., Liugen, K., Hui, H., Zhongfan, W., 2006, The role of calcium in microstructural refinement of AZ91 magnesium alloy. *Journal of Wuhan University of Technology-Mater. Sci. Ed.*, 21(4): 45-47, doi:10.1007/BF02841202.
- Sonar, T., Lomte, S., Gogte, C., 2018, Cryogenic Treatment of Metal – A Review. *Mater. Today-Proc.*, 5(11, Part 3): 25219-25228, doi:<https://doi.org/10.1016/j.matpr.2018.10.324>.
- Tolnai, D., Subroto, T., Gavras, S., Buzolin, R., Stark, A., Schell, N., Hort, N., 2018, Phase Formation during Solidification of Mg-Nd-Zn Alloys: An In Situ Synchrotron Radiation Diffraction Study. *Materials (Basel, Switzerland)*, 11(9): 1637, doi:10.3390/ma11091637.
- Wang, Y., Liao, B., Liu, J., Chen, S., Feng, Y., Zhang, Y., Zhang, R., 2012, Effects of deep cryogenic treatment on the solid-state phase transformation of Cu–Al alloy in cooling process. *Phase Transit.*, 85(7): 650-657, doi:10.1080/01411594.2012.659738.
- Yan, H., Wang, Z., 2016, Effect of heat treatment on wear properties of extruded AZ91 alloy treated with yttrium. *J. Rare Earth*, 34(3): 308-314, doi:[https://doi.org/10.1016/S1002-0721\(16\)60030-3](https://doi.org/10.1016/S1002-0721(16)60030-3).

REFERENCES (continue)

Zafari, A., Ghasemi, H.M., Mahmudi, R., 2014, An investigation on the tribological behavior of AZ91 and AZ91+3wt% RE magnesium alloys at elevated temperatures. *Mater. Design*, 54: 544-552, doi:<https://doi.org/10.1016/j.matdes.2013.08.073>.

Zheng, L., Nie, H., Liang, W., Wang, H., Wang, Y., 2016, Effect of pre-homogenizing treatment on microstructure and mechanical properties of hot-rolled AZ91 magnesium alloys. *J. Magnes. Alloy*, 4(2): 115-122, doi:<https://doi.org/10.1016/j.jma.2016.04.002>.